CHAPTER 2

THE STATE OF THE OCEAN

This chapter includes an overview of the current state of knowledge about ocean climate in FY 2004, placed in historical context. Expert scientists who monitor, observe, and analyze the ocean products described in this chapter (e.g., sea level, ocean carbon, SST) have produced concise summaries describing why it is important to monitor these variables. Climate applications are presented along with an explanation of how the observing system needs to be enhanced to improve ocean analysis and reduce present uncertainties. This chapter focuses primarily on decision makers and non-scientists interested in, and concerned about, ocean research.

The short articles presented in this chapter describe the products listed in Table 2.1 and are the result of ocean projects funded, in whole or in part, by NOAA's Office of Climate Observation.

Table 2.1. Products

2.1 Global sea level rise to identify changes resulting from climate variability – *Laury Miller and Bruce Douglas*

2.2 Sea surface temperature to identify significant patterns of climate variability – *Richard Reynolds*

2.3 Ocean heat and fresh water content and transports to identify where anomalies enter the ocean, how they move and are transformed, and where they re-emerge to interact with the atmosphere. Identify the essential aspects of thermohaline circulation and the subsurface expressions of the patterns of climate variability – *Lynne Talley*

2.4 Evolution of the 2004 El Niño and heat content variations – *Michael McPhaden*

2.5 Global ocean carbon cycle: inventories, sources and sinks – *Richard Feely and Rik Wanninkhof*

2.6 Surface current observations to identify significant patterns of climate variability – *Peter Niiler and Nikolai Maximenko*

2.7 Air-sea exchange of heat, fresh water, momentum to identify changes in forcing functions driving ocean conditions and atmospheric conditions – *Robert Weller*

2.8 Sea ice extent and thickness – *Ignatius Rigor and Jackie Richter-Menge*

2.1 GLOBAL SEA LEVEL RISE

by Laury Miller[1], Bruce C. Douglas[2]

[1]Laboratory for Satellite Altimetry, NOAA/Lab for Satellite Altimetry, Silver Spring, MD
[2]Florida International University/Lab for Coastal Research, Miami, FL

Satellite altimeter observations since 1993 show global sea level rising almost steadily at rate of 2.8 +/-0.4 mm/year (Fig. 1). This trend is significantly higher than the 20th century rate of 1.8 +/-0.3 mm/year determined from tide gauge observations made over the past 50 to 100 years (Douglas 1997; Peltier 2001; Miller and Douglas 2004; Church et al. 2004; Holgate and Woodworth 2004; White et al. 2005). However, it is unclear whether the increased rate observed by satellite altimeters reflects a long-term change with respect to the historical rate or some manifestation of decadal variability.

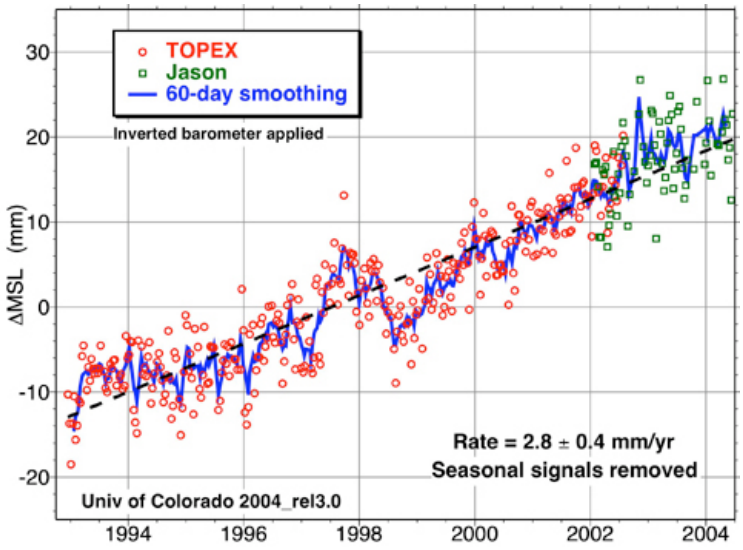

Figure 1. Global mean sea level variations determined from TOPEX and Jason-1 satellite altimeter observations.

A map of the altimeter-measured trends (Fig. 2) shows that all of the ocean basins experienced rising levels over the past decade, but large regional variations are also evident. The tropical western Pacific and Southern Oceans exhibit high positive trends (>10 mm/year), while the Northern Pacific is distinctly negative. The geographical pattern of trends is roughly similar to that observed in upper ocean heat content change as determined from *in-situ* hydrographic measurements (Cabanes et al. 2001) suggesting that, at least on decadal time scales, regional sea level trends are largely controlled by thermal processes. Global mean warming of the upper 750 m of the water column can account for 1.6 +/-0.2 mm/yr of global sea level change between 1993 and 2003 (Willis et al. 2004). This contrasts sharply with the average 20th century contribution to sea level rise from thermal expansion, estimated to be about 0.5 mm/yr (Antonov et al. 2002). The remaining portion of the total trend for the past decade, roughly 1.2 mm/year, is likely to have come from the melting of grounded ice on Greenland and/or Antarctica and, to a lesser extent, from mountain glaciers, a result consistent with the average 20th century mass contribution to sea level rise estimated by Miller and Douglas (2004). The true significance of the recent increased thermosteric contribution to sea level rise can only be determined by continuing altimetric and *in-situ* (e.g., ARGO) observations.

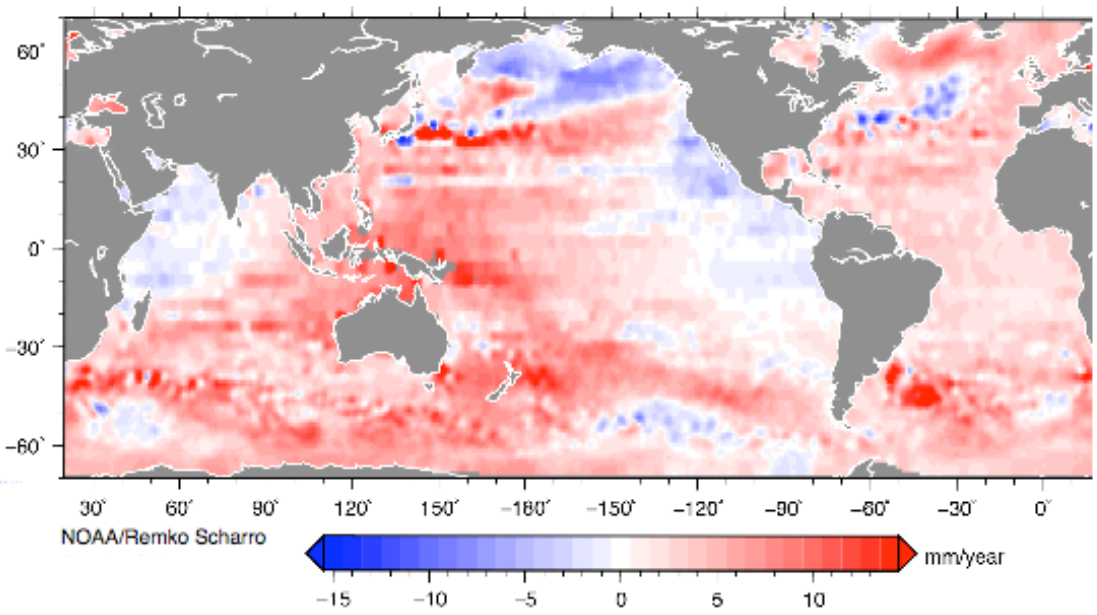

Figure 2. Sea level trends over 1993-2004 determined from TOPEX *and* Jason-1 satellite altimeter observations. The global mean of this map gives the 2.8 mm/yr value shown in Fig. 1.

References

Antonov, J.I., S. Levitus, and T.P. Boyer, 2002: Steric sea level variations during 1957-1994: Importance of salinity, *J. Geophys. Res.*, **107**, C12, 8103, doi:10.1029/2001JC000964.

Cabanes, C., A. Cazenave, and C. LeProvost, 2001: Sea level rise during the past 40 years determined from satellite and in-situ observations, *Science*, **294**, 840-842.

Church, J.A., N.J. White, R. Coleman, K. Lambeck, and J.X. Mitrovica, 2004: Estimates of the regional distribution of sea level rise over the 1950-2000 period, *J. Climate,* **17**, 2609-2624.

Douglas, B.C., 1997: Global sea rise: A redetermination, *Surveys in Geophys.,* **18**, 279-292.

Holgate, S.J., and P.L. Woodworth, 2004: Evidence for enhanced coastal sea level rise during the 1990's, *Geophys. Res. Lett.*, **31**, doi:10.1029/2004GL019626.

Miller, L., and B.C. Douglas, 2004: Mass and volume contributions to 20th-century global sea level rise, *Nature,* **428**, 406-409.

Peltier, W.R., 2001: Global glacial isostatic adjustment and modern instrumental records of relative sea level history, in *Sea Level Rise, History and Consequences*, edited by B.C. Douglas, M.S. Kearney, and S.P. Leatherman, 65-95, Academic, San Diego, Calif.

White, N.J., J.A. Church, and J.M. Gregory, 2005: Coastal and global averaged sea level rise for 1950 to 2000, *Geophys. Res. Lett.,* **32**, L01601.

Willis, J.K., D. Roemmich, and B. Cornuelle, 2004: Interannual variability in upper ocean heat content, temperature, and thermosteric expansion on global scales, *J. Geophys. Res.,* **109,** C12036.

2.2 SEA SURFACE TEMPERATURES IN 2004

by Richard W. Reynolds, National Climatic Data Center, Asheville, North Carolina

The purpose of this section is to discuss sea surface temperatures for 2004. This will include comparisons to other years, primarily 2000-2003. The analysis used is the weekly optimum interpolation (OI) analyses of Reynolds et al. (2002). The analysis uses ship and buoy in situ SST data as well as satellite SST retrievals from the infrared (IR) Advanced Very High Resolution Radiometer (AVHRR). The AVHRR was first available in November 1981, so the analysis begins in that month. The results will be shown as anomalies which are the defined as differences from a 1971-2002 climatological base period using methods described by Xue et al. (2003). Anomalies are used to best separate climate signals from the annual mean and seasonal cycle. In many of the figures which follow, monthly fields are used. The monthly fields are derived by interpolating the weekly fields to the day of the month and then averaging the daily values in the appropriate month. This was done to smooth the results so that the climate signal can more easily be extracted from the weekly variability.

To best demonstrate the overall changes between 2004 and other years, time series of the average monthly OI SST anomaly from 75ºS to 75ºN is shown for the entire period of record (Fig. 1).

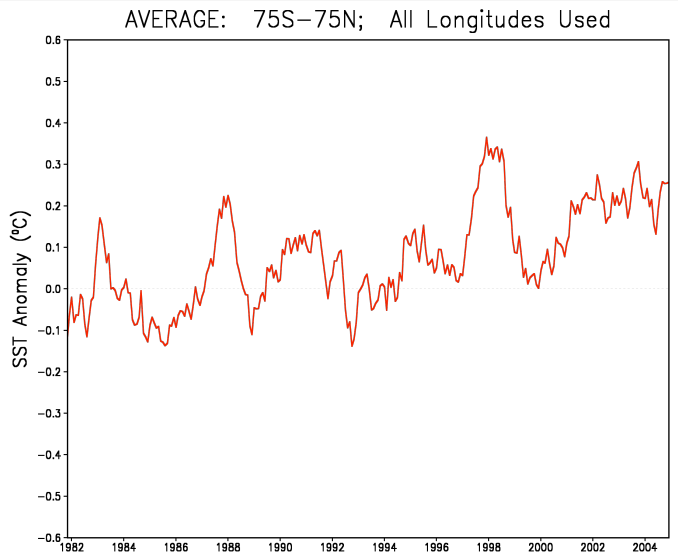

Figure 1. Time series of average monthly SST anomalies between 75ºS and 75ºN for the period November 1981 through December 2004. The anomalies are computed relative to a 1971-2000 base period.

The general change over this period is a slow warming with some large fluctuations of 1 to 3 years. Please recall that the climatological base period is 1971-2000 so the overall warming tends to favor positive over negative anomalies toward the end of the record. The 1 to 3 year fluctuations are usually due to the warm and cold SST anomalies in the tropical Pacific due to large El Niño and large La Niña events, respectively. The impacts of these events often influence the tropical Indian SST anomalies and may influence the tropical Atlantic SST anomalies. For example, the El Niño event of 1982-83 occurred along with cold tropical Atlantic SST anomalies while the El Niño event of 1997-98 occurred along with warm tropical Atlantic SST anomalies. However, the SST anomaly curve is relatively flat from 2001 through 2004. This suggests overall warming trends were small over this period and that no large El Niño or La Niña events occurred.

To now focus on the changes during 2004, the mean and standard deviation of the weekly anomaly for 2004 is shown in Figure 2. The mean anomalies in the upper panel show warm anomalies in the Central Pacific, the North Atlantic and to a weaker extent, the tropical Indian Ocean and the western Indian Ocean near 35ºS. The standard deviation of the anomaly in the lower panel shows the strongest variability between roughly 30ºN and 70ºN and in the eastern

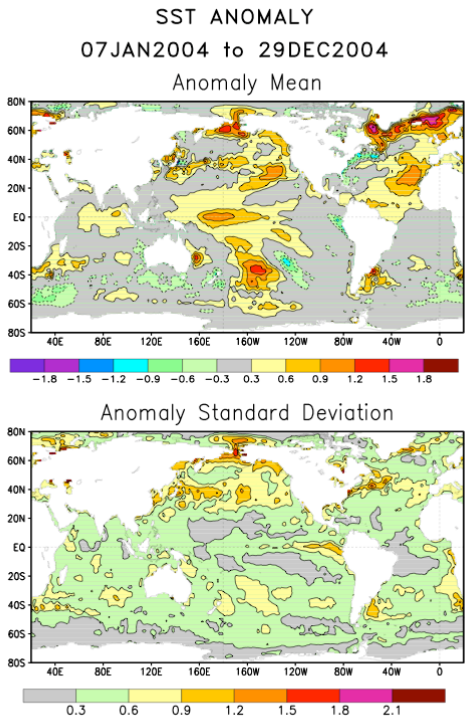

Figure 2. Mean and standard deviation of weekly SST anomalies for the period 7 January 2004 through 29 December 2004. The anomalies are computed relative to a 1971-2000 base period. The contour interval is 0.3ºC; the 0 contour is not shown.

Tropical Pacific. In addition, there is more modest variability along the equator in the eastern Pacific and between 30ºS and 50ºS east of South America and both east and west of the Cape of Good Hope. To determine the similarity between 2003 and 2004, the 2003 weekly mean and standard deviation is shown in Figure 3. The figures show that the 2003 and 2004 standard deviations (lower panels) are very similar. The anomaly patterns (upper panels) are also similar with important differences in the eastern Pacific near 40ºN and in the South Atlantic especially near 20ºS.

It would be useful to also consider climate indices. However, the North Atlantic Oscillation, the Arctic Oscillation, the Pacific North American Pattern and the Antarctica Oscillation are expressed in terms of sea level pressure and these patterns are not confined to oceanic regions (see "teleconnections" on
http://www.cpc.ncep.noaa.gov/products/precip/CWlink/MJO/climwx.shtml
and http://www.ncdc.noaa.gov/oa/climate/research/teleconnect/teleconnect.html).

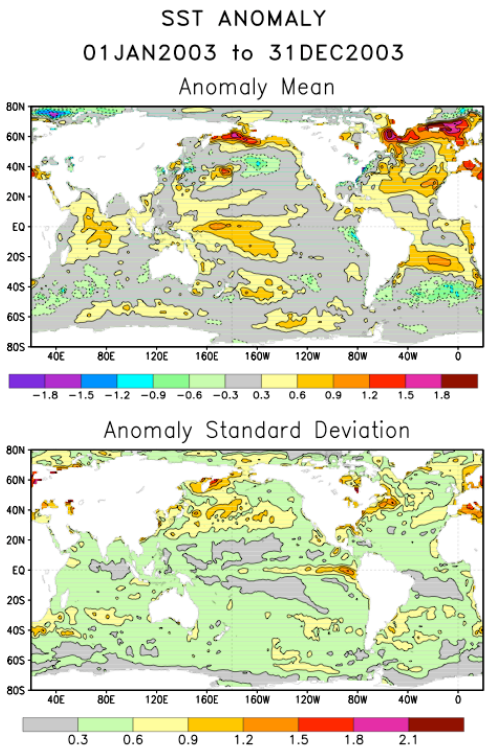

Figure 3. Mean and standard deviation of weekly SST anomalies for the period 1 January 2003 through 31 December 2003. The anomalies are computed relative to a 1971-2000 base period. The contour interval is 0.3ºC; the 0 contour is not shown.

Thus, SSTs alone cannot define these indices. The relationship between sea level pressure and SST is better defined for El Niño and La Niña events. However, that will be discussed elsewhere in this report. The Pacific Decadal Oscillation (PDO) is defined in terms of SST (see http://tao.atmos.washington.edu/pdo/ and Mantua, et al, 1997). The PDO needs to be measured on annual and longer scales. A plot of the annual PDO for 1982 through 2004 (not shown) is noisy with a PDO value for 2004 is 0.11 which too close to zero to be significant.

To investigate the variations in 2004, the zonal monthly anomalies are examined for two longitude bands with large anomalies as suggested by Figure 2. The first zonal band is for the central Pacific (160ºE to 120ºW) and is shown in Figure 4 for 2000-2004. The region with the highest variability occurs along 60°N. There the anomalies are near normal from January 2000 until June 2002. For almost all of the remaining period (July 2002 through December 2004) the anomalies are above normal with especially strong anomalies for two periods of about 5 months each which are centered on July 2003 and July 2004. (Please note that the region of high variability near 65ºN, Bering Strait, is due to the limited ocean area for the average.) The other

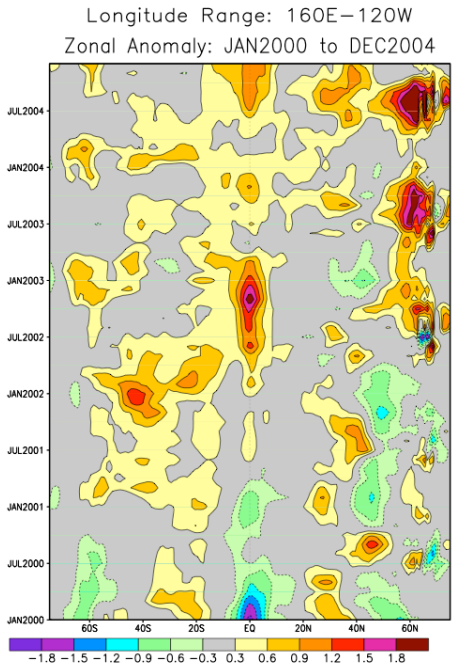

Figure 4. Zonal mean SST anomalies averaged between 160ºE and 120ºW (the Central Pacific) for the period January 2000 through December 2004. The anomalies are computed relative to a 1971-2000 base period. The contour interval is 0.3ºC; the 0 contour is not shown.

region with high variability occurs along the equator where the end of a La Niña event is evident in early 2000. This event is followed by an El Niño event in 2002-2003 and the beginning of a new El Niño event in the second half of 2004. The large positive anomaly (Fig. 2) centered near 40ºS and 160ºW is not strongly evident here even though it persisted through both 2003 and 2004. This was because it was often offset by nearby negative anomalies along the same latitude (Fig. 2).

The second zonal band is for the Atlantic (80ºW- 0º) for 2000-2004 (Fig. 5). Here the band of highest variability is centered on about 60ºN. It tends be above normal for the entire period with a tendency of peak warming during August through September. The size of these peaks becomes largest in 2003 and 2004 closely matching the variability found in the North Pacific along this same latitude band. The remaining features are less coherent. The warm anomaly in 2004 near 20ºN and 20ºW (Fig. 2) was primarily for the second half of 2004 and is suggested by the Fig. 5. However, it appears weaker because the zonal average is for the entire Atlantic while the anomaly is confined to the eastern half of the Atlantic.

The most important extra tropical SST variability for 2004 occurs in both 2003 and 2004 along 60ºN and with larger values between August and October. This is shown in Fig. 6 by the time series of the average weekly OI SST anomaly from 50ºN to 70ºN for 2003 and 2004. These summer and fall warm SST anomalies are the oceanic response to large summer and fall warm land surface air temperatures anomalies found along this same latitude band (see http://www.ncdc.noaa.gov/oa/climate/research/monitoring.html).

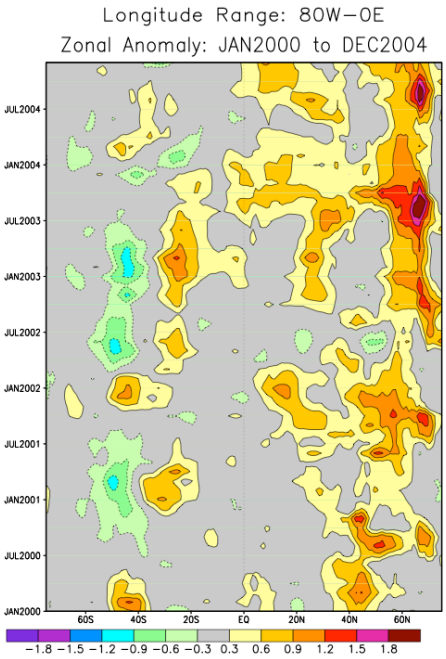

Figure 5. Zonal mean SST anomalies averaged between 80ºW and 0º (the Atlantic) for the period January 2000 through December 2004. The anomalies are computed relative to a 1971-2000 base period. The contour interval is 0.3ºC; the 0 contour is not shown.

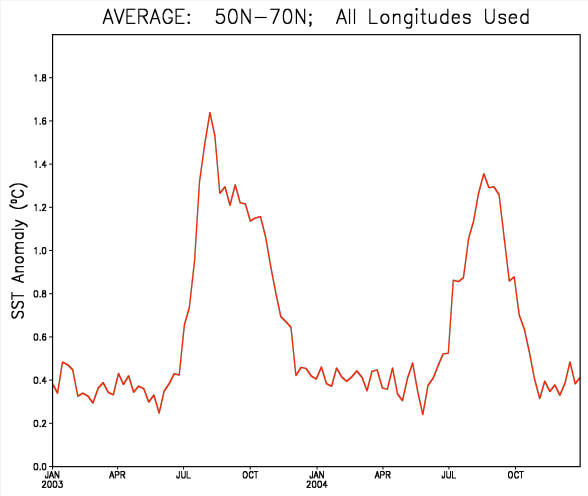

Figure 6. Time series of average weekly SST anomalies between 50ºN and 70ºN for the period 1 January 2003 through 29 December 2004. The anomalies are computed relative to a 1971-2000 base period.

References

Mantua, N.J. and S.R. Hare, Y. Zhang, J.M. Wallace, and R.C. Francis, 1997: A Pacific interdecadal climate oscillation with impacts on salmon production. *Bull. Am. Meteorol. Soc.*, **78**, 1069-1079.

Reynolds, R. W., N. A. Rayner, T. M. Smith, D. C. Stokes and W. Wang, 2002: An improved in situ and satellite SST analysis for climate. *J. Climate*, **15**, 1609-1625.

Xue, Y., T. M. Smith, and R.W. Reynolds, 2003: A new SST Climatology for the 1971-2000 Base Period and Interdecadal Changes of 30-Year SST Normal. *J. Climate*, **16**, 1601-1612.

2.3 OCEAN HEAT AND FRESH WATER CONTENT AND TRANSPORTS

by Lynne Talley, Scripps Institution of Oceanography, La Jolla, California

2.3.1 Introduction

Heat and freshwater transport changes as well as changes in local air-sea exchange are recorded in variations in ocean temperature and salinity distributions. Highlighted results are given in section 2.3.2.

Global fields and anomalies of SST for 2004 are shown in Section 2.3.3. No global surface salinity products are available for 2004, although the data sets that could be used to produce them are accruing.

Section 2.3.4 summarizes changes in the upper ocean through 2004, including variations in the tropical Atlantic and Indian Oceans, and Pacific Decadal Oscillation and North Atlantic Oscillation variations in the Pacific and Atlantic.

Section 2.3.5 describes temperature, salinity and transport variations in waters affected by the global overturning circulation. Variations in deep and bottom waters formed in the Antarctic are also described. In section 2.3.6, a new analysis of heat content change from 1993 to 2003 is reviewed.

2.3.2 Some highlights

(1) Sea surface temperature in 2004 was higher than the long-term mean (1968-1996) over most of the globe, with the greatest increases in the Arctic. Alternating cooling and warming regions occupy the far southern hemisphere. Temperature increases in most of the oceans are less than 0.5°C, but are much greater in the polar latitudes (> 4°C). A large cooled patch south of Africa also had relatively large departures from the mean (more than 2°C colder than the mean).

(2) Heat content calculated from combined data sets increased monotonically from 1993 to 2003.

(3) Freshening in the high latitude North Atlantic continued into 2004.

2.3.3 Global upper ocean temperature and salinity

Annual mean and monthly anomalies of sea surface temperatures for 2004 are shown in Figure 1 (NCEP/NCAR reanalysis). Sea surface salinity analyses are much more difficult to find; the EU's Coriolis project produces maps for the Atlantic based on profiling ARGO data, but there is no global product. The U.K. Met Office global Forecasting Ocean Assimilation Model (FOAM) also produces surface salinity maps, but access is no longer available without charge.

Surface temperature is higher than the long-term mean (1968-1996) over most of the northern hemisphere and tropics. In most ocean basins, the excess is less than 0.5°C. The greatest extremes are found at polar latitudes. In the Arctic, the temperature is more than 4°C higher than the mean along the northern coast of Alaska and eastern Siberia, and around Greenland eastward to Svalbard and Russia. Major regions of cooler temperatures are restricted to the southern hemisphere, with the largest cooled region in a large patch of the Antarctic south of Africa. Alternating patches of warmed and cooled water are found around Antarctica, with warming in the Weddell Sea, along Queen Adelie Land, and in the northern Ross Sea. Within the southern hemisphere ocean basins, all three oceans show cooling in the east and warming in the west, which is consistent with an increase in strength of the subtropical gyres.

Global maps of upper ocean heat content and subsurface temperature anomalies for 2004 are apparently not publicly available. (Products from JEDAC that were used for the State of the Ocean 2003 report were discontinued in 2004.) New global heat content maps (Willis et al. 2004) showing decadal trends are presented in section 2.3.7.

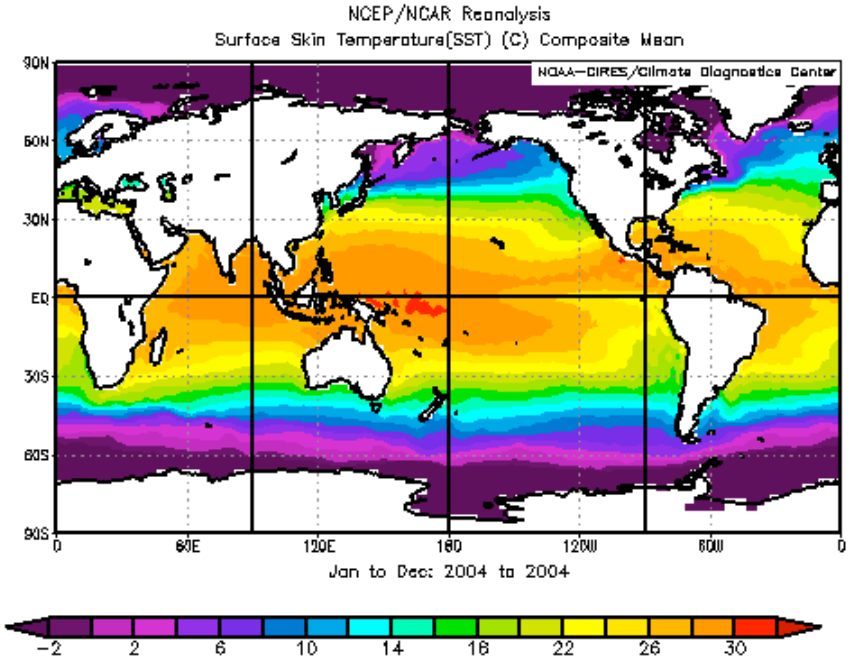

(a)

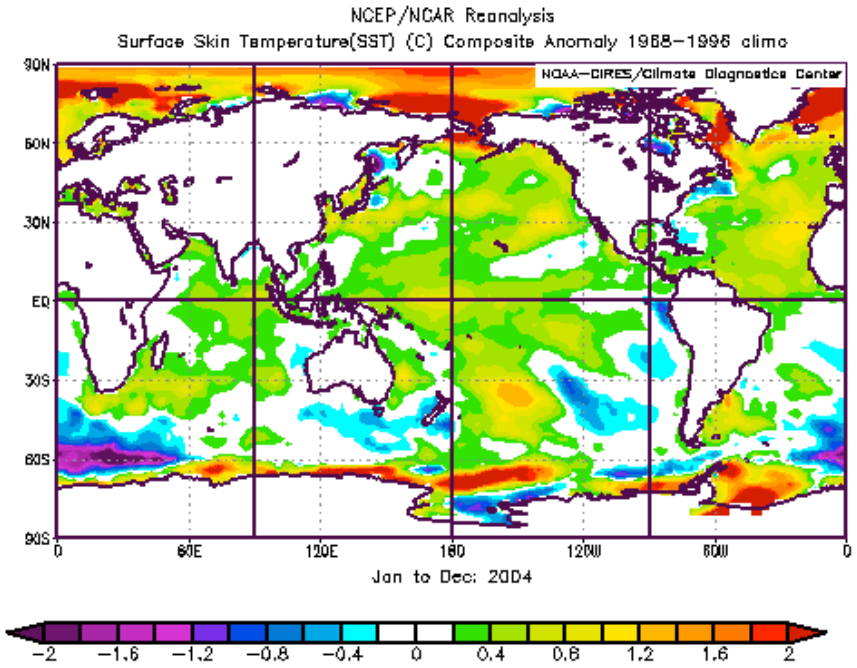

(b)

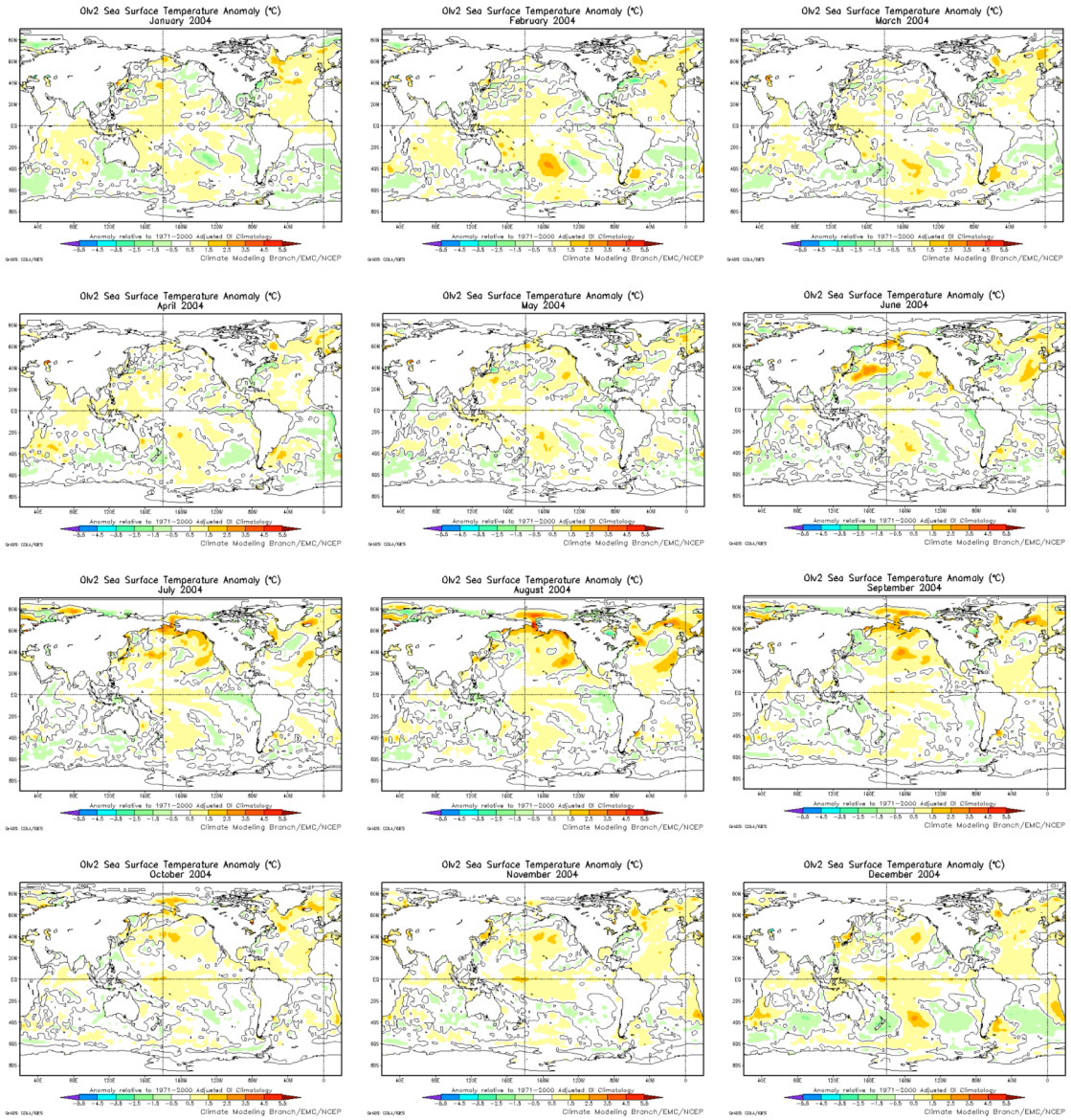

Figure 1. (a) Annual mean sea surface temperature and (b) anomaly from the 1968-2000 mean, for 2004 (NCEP/NCAR reanalysis). (http://www.cdc.noaa.gov/Composites/) (c) Monthly SST anomalies for 2004 from the 1971-2000 mean (Reynolds et al. 2002) (http://www.emc.ncep.noaa.gov/research/cmb/sst_analysis/)

Subsurface temperature is monitored through the XBT program (since the 1970s) and more recently from the ARGO profiling float program, with underwent rapid expansion in 2004 (Fig. 2). All non ice-covered basins are now instrumented with ARGO floats, although many regions are still undersampled. Implementation grew to the 50% level in late 2004. Operational products of subsurface temperature and salinity fields are being produced for the Atlantic (examples of salinity maps in Fig. 3), and of subsurface temperature for the North Pacific (examples in Fig. 5). Anomaly maps are apparently not yet available.

No operational global maps of surface or upper ocean salinity anomalies for 2004 are available. Salinity maps for the Atlantic Ocean are now being produced by the European Union's Coriolis

project (Fig. 3) using ARGO data, but this is a fledgling effort as of now, covering neither the globe nor including salinity anomalies.

Because salinity impacts decadal and longer climate variability, and because of the use of salinity as a signature of such climate variability, it is imperative that regular salinity products be compiled and made publicly available as soon as possible. To be most useful, both the observed and anomaly fields should be shown. A fast turnaround taxes the ability to calibrate salinity observations in near real-time, and so products with some lag time would clearly be desirable.

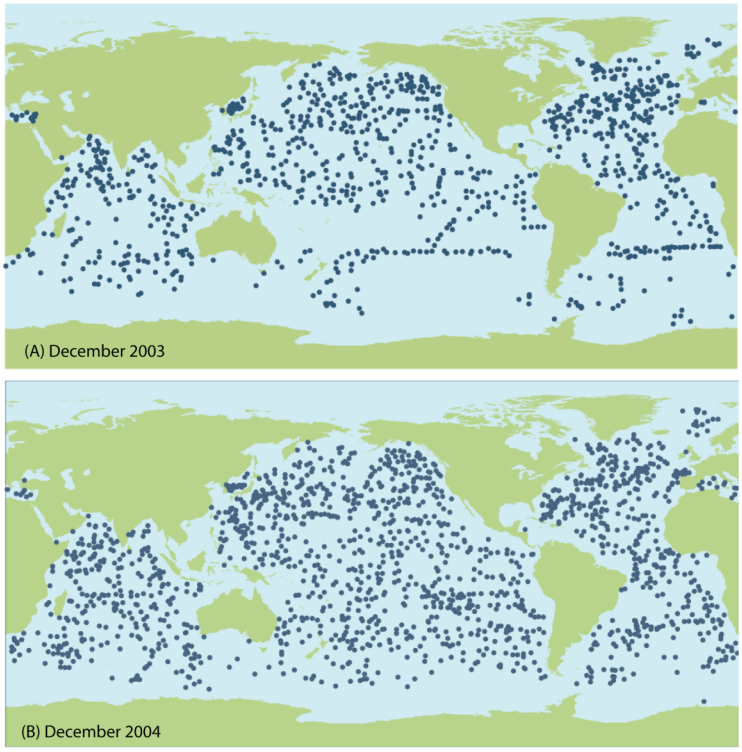

Figure 2. ARGO floats in December 2003 and December 2004 (http://www.jcommops.org).

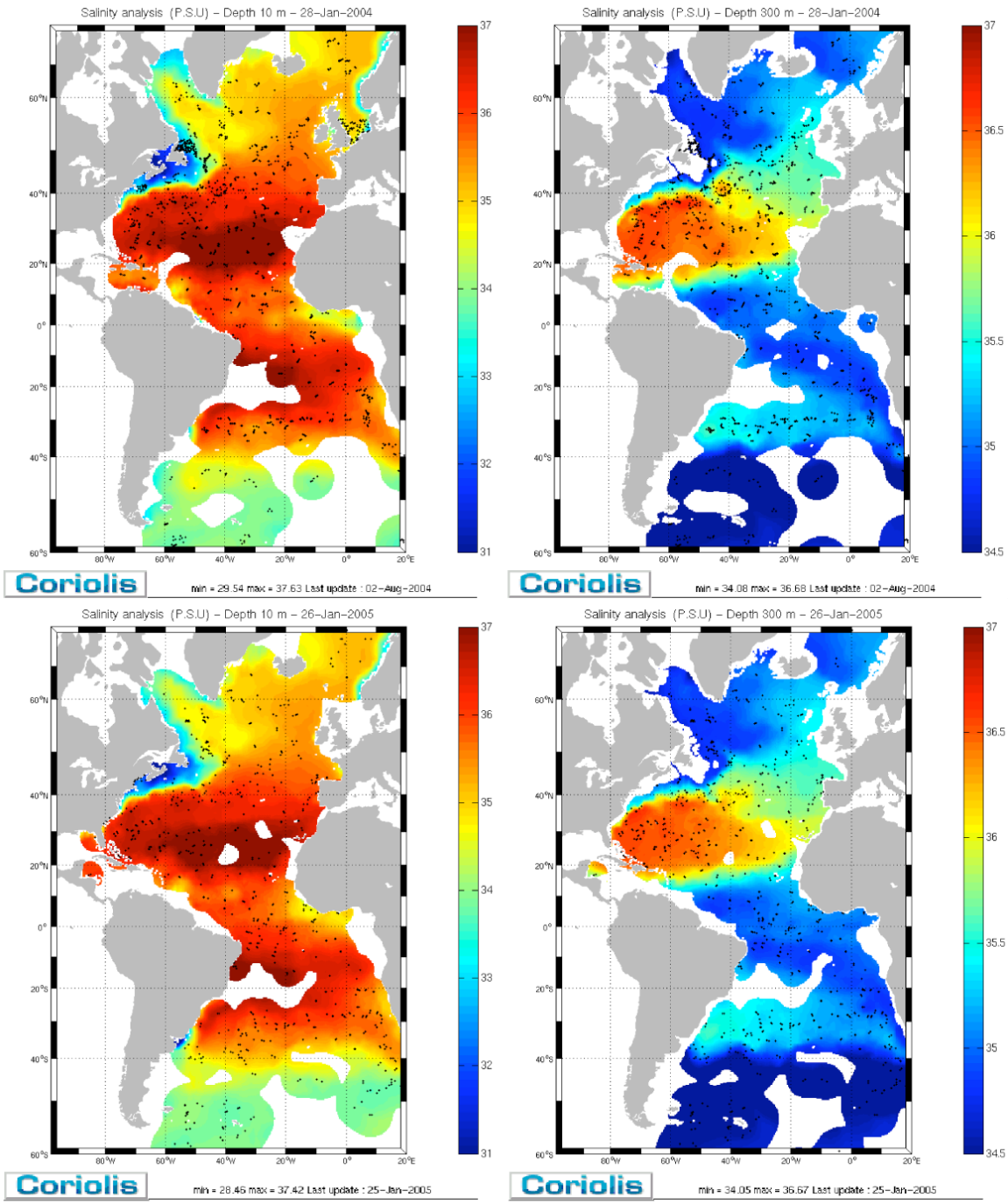

Figure 3. Salinity at 10m and 300 m in late January 2004 and January 2005, based on ARGO float data, from the Coriolis operational oceanography (http://www.coriolis.eu.org/coriolis/cdc/atlantic_area.htm). Maps are available at other depths, as are temperature maps.

2.3.4 Basin-scale upper ocean variations

Upper ocean variations in temperature, salinity and circulation are strongly associated with the natural modes of variability, variously identified as El Nino Southern Oscillation (ENSO), the Pacific Decadal Oscillation (PDO) (section 2.3.4.1), the tropical Atlantic dipole, the Indian dipole

(both in 2.3.4.2), the Southern Annular Mode (SAM) (including the Antarctic Circumpolar Wave or Antarctic Dipole Mode) (2.3.4.3), and the North Atlantic Oscillation (NAO) and Arctic Oscillation (AO) (or Northern Annular Mode) (2.3.4.4). The ocean response in 2004 to the modes is reviewed in this section.

2.3.4.1. Upper ocean property variations in the mid-latitude Pacific and mid-latitude southern hemisphere

The extratropical Pacific and subtropical regions of the southern hemisphere respond to several identified climate modes. The Pacific Decadal Oscillation (PDO) (Fig. 4) (Zhang et al. 1997; Mantua et al. 1997) is a realization of the dominant Pacific mode, although recently it has been suggested that it is a combination of ENSO and the PNA mode (Aleutian Low strength) (Schneider and Cornuelle 2004). The PDO is meridionally symmetric about the equator. When the index is high, the tropical Pacific is warm and the high latitude Pacific is cold, and vice versa. A high PDO index is also associated with high pressure in the tropical Pacific and low pressure in the higher latitudes (deep Aleutian low). The PDO spatial pattern is similar to that of ENSO, but without the very large peak in amplitude in the tropics. The PDO thus modulates the strength of ENSO; when the PDO index is high, ENSO is especially pronounced. Boundary regions bordering continents are especially impacted by PDO-variations in the ocean, with impacts on marine-based economics (fisheries) and coastal climate. When the PDO index is high, circulation in the Gulf of Alaska is stronger and less subpolar water enters the California Current. The Oyashio is also strong during high PDO.

The PDO was high in 2004, continuing from mid-2002. This followed a short period of low PDO (1998-2002), preceded by a prolonged period of high PDO, which began in 1976. Because of the relatively long duration in any particular phase and because of the widespread ecological impacts of the PDO, much attention has been focused on identifying "regime shifts" such as that in 1976 as they happen, although a true shift can only be defined several (5 to 10) years after the fact.

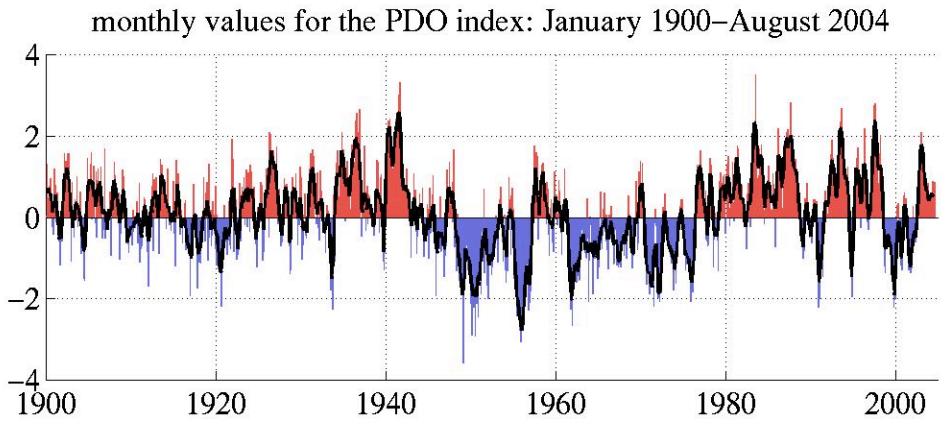

Figure 4. Pacific Decadal Oscillation index (http://tao.atmos.washington.edu/pdo/).

SST anomalies in 2004 (Fig. 1) generally showed the warm PDO phase, with warm eastern tropical waters and colder mid-latitude centers. The pattern also matches that of ENSO; the year 2004 continued a weak ENSO. The ENSO changes are apparent in the sample North Pacific temperature maps constructed from ARGO and XBT data (Fig. 5), with warmer equatorial waters at the end of 2004 and an eastward shift of the warmest water at 100 m to the central Pacific.

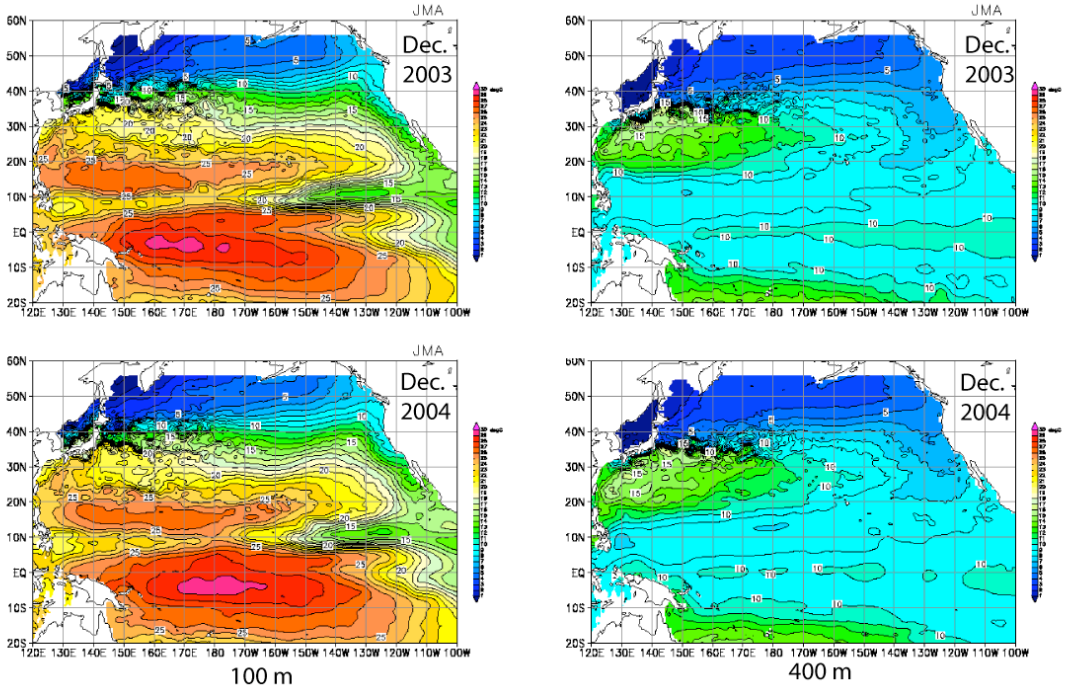

Figure 5. Examples of monthly sub-surface temperature analysis (available from surface down to 400 m), for December 2003 and December 2004, at 100 and 400 m, from the Japan Meteorological Agency, incorporating ARGO and XBT data (http://argo.kishou.go.jp/index.html).

A detailed repeated hydrographic section from east to west across the mid-latitude North Pacific occupied in summer 2004, as part of the U.S. Repeat Hydrography program for CLIVAR/CO, showed warming through the subtropical gyre, down into the thermocline (Robbins, personal communication) (Fig. 6).

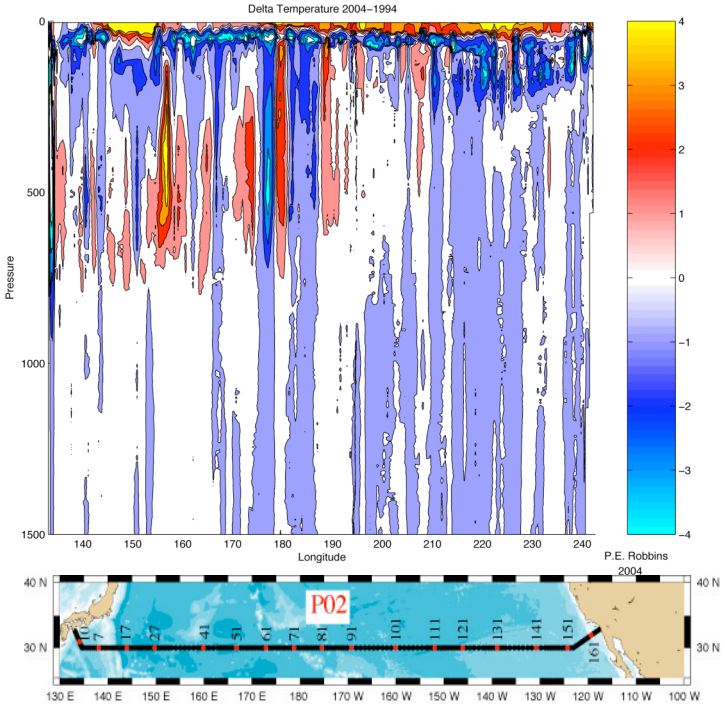

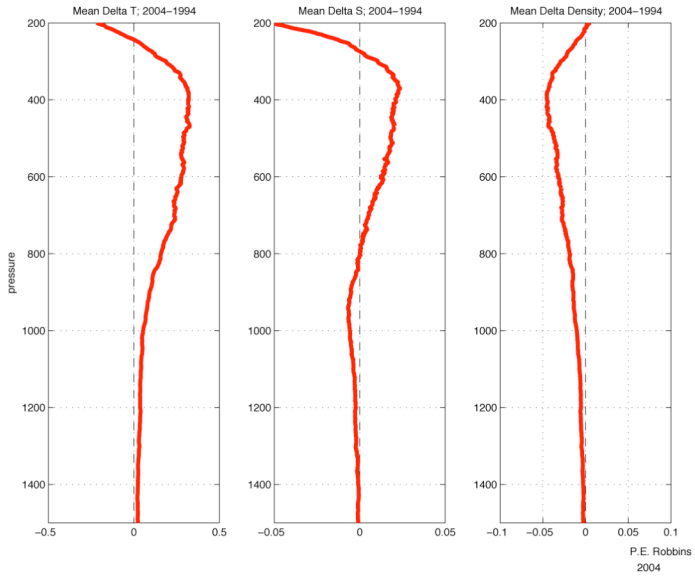

Figure 6. (a) Temperature change, (b) station locations, and (c) integrated temperature, salinity and potential density change, for hydrographic section occupied in 2004 minus another in 1994. (Robbins, personal communication).

2.3.4.2. Tropical Atlantic and Indian Oceans

The tropical regions of the Atlantic and Indian Ocean are influenced by upper ocean variations that might be separate from ENSO, although lagged ENSO response is also apparent. The tropical Atlantic experiences variability that has been described in terms of either a cross-equatorial dipole or as nearly independent modes north and south of the equator. There is no regularly produced index of a dipole or gradient mode. The Climate Diagnostics Center and Climate Diagnostics Bulletin (CDB) report separate Tropical North Atlantic (TNA) and Tropical South Atlantic (TSA) mode indices (Fig. 7).

The North and tropical Atlantic and the tropical Indian Ocean were anomalously warm throughout 2004 relative to a 1968-1996 mean (Fig. 1). The Atlantic warmth is reflected in continuing positive values of the TNA through 2004 (Fig. 6).

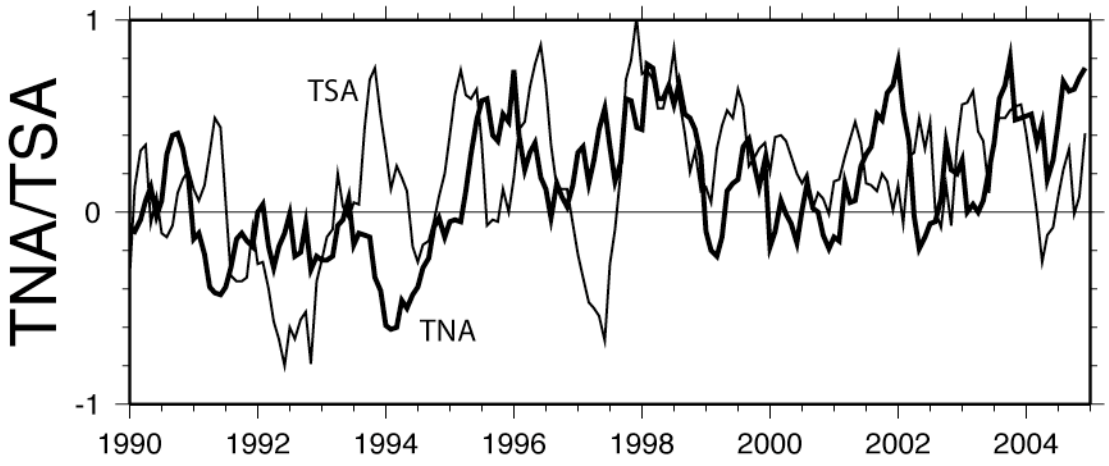

Figure 7. (a) Tropical North Atlantic (TNA - heavy) and Tropical South Atlantic (TSA - light) indices, including 2004. From the NOAA Climate Diagnostics Center (http://www.cdc.noaa.gov/ClimateIndices/Analysis/).

High density XBT sections are occupied across all oceans approximately seasonally, with profiling to more than 800 m depth and close station spacing to produce the highest quality volume transport estimates. As years of data accumulate, it will be possible to track interannual and then decadal variations in upper ocean temperature structure using these data. The Atlantic high density network maintained by NOAA is shown in Figure 8, with a sample section from line AX8.

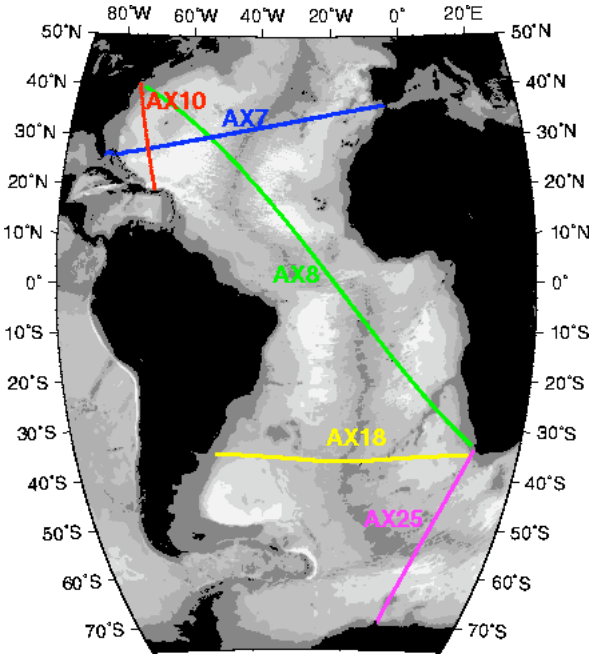

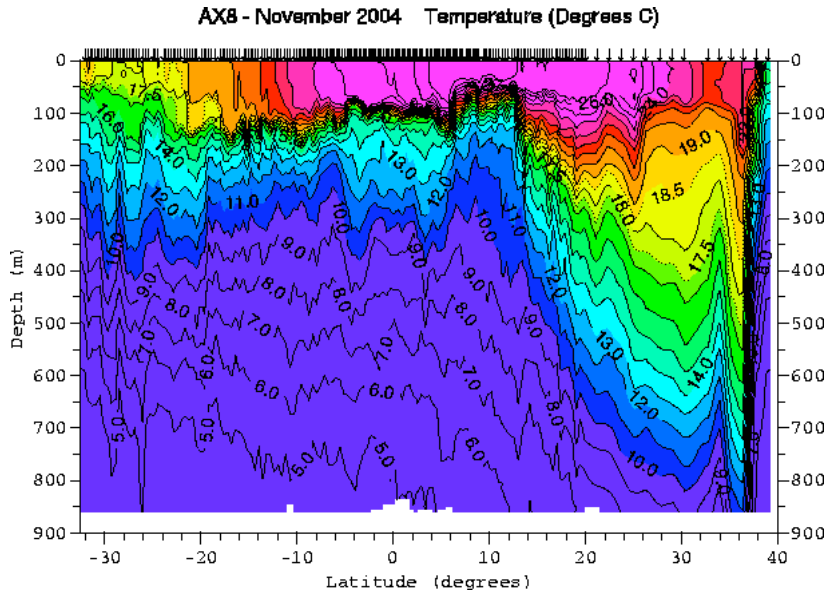

Figure 8. (a) High density XBT network maintained by NOAA AOML, with sections 4 times per year. (b) Sample section along AX8 (November 2004).
(http://www.aoml.noaa.gov/phod/hdenxbt/)

Indian Ocean variability has been described in terms of a dipole mode (Saji et al. 1999) (Fig. 9), although Indian variability is also heavily influenced by ENSO.

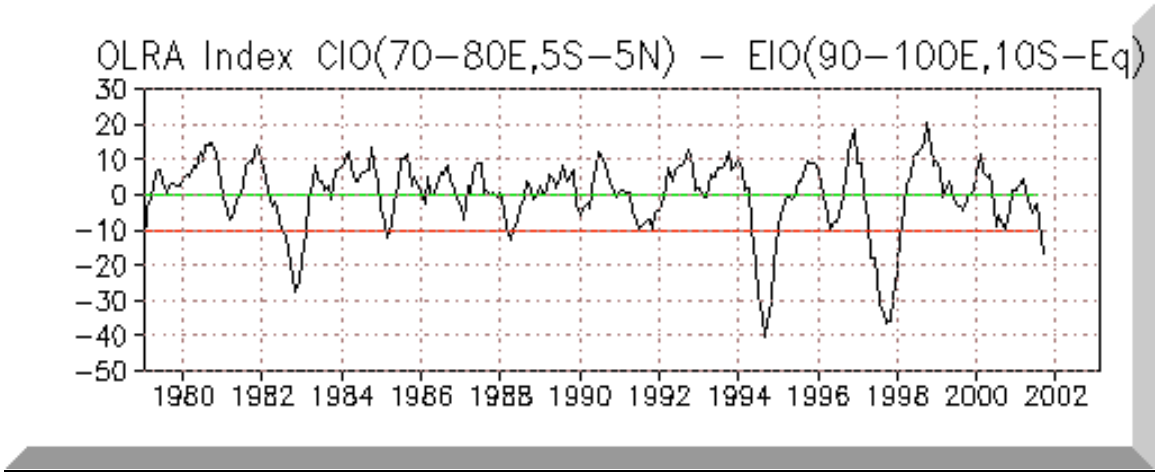

Figure 9. Indian Dipole Index, based on OLR (Saji et al. 1999)
(http://www.jamstec.go.jp/frsgc/research/d1/iod/dmi.html).

2.3.4.3. Southern Hemisphere Annular Mode

The Southern Hemisphere Annular Mode (SAM) or Antarctic Oscillation (AAO) is the major decadal mode of climate variation in the southern ocean (Thompson and Wallace 2001). When the SAM index is high, the westerly winds are shifted to the south and are stronger; that is, the polar vortex is spun up. The associated Antarctic temperature changes are a colder interior of the continent and warmer region in the Antarctic Peninsula and ocean in the area of the Subantarctic Front. The AAO is tracked by the Climate Prediction Center (Fig. 10).

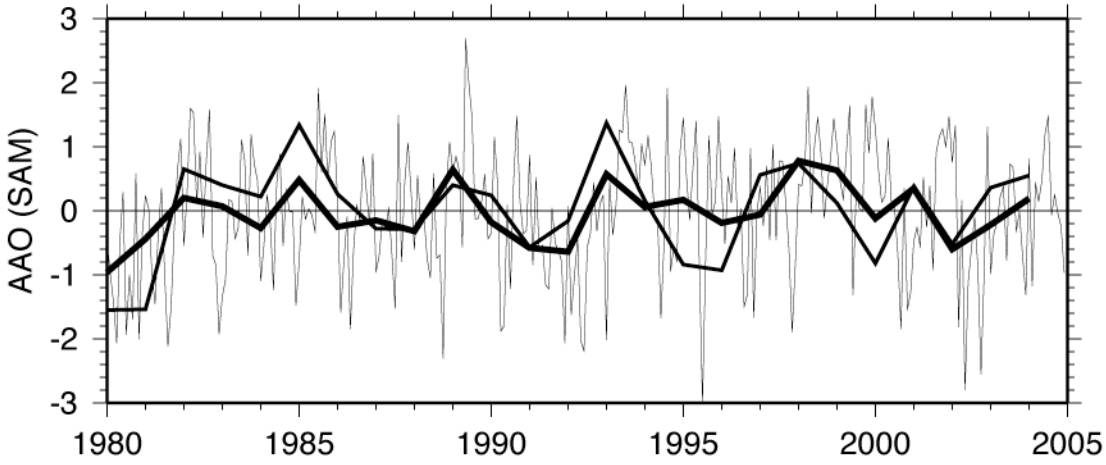

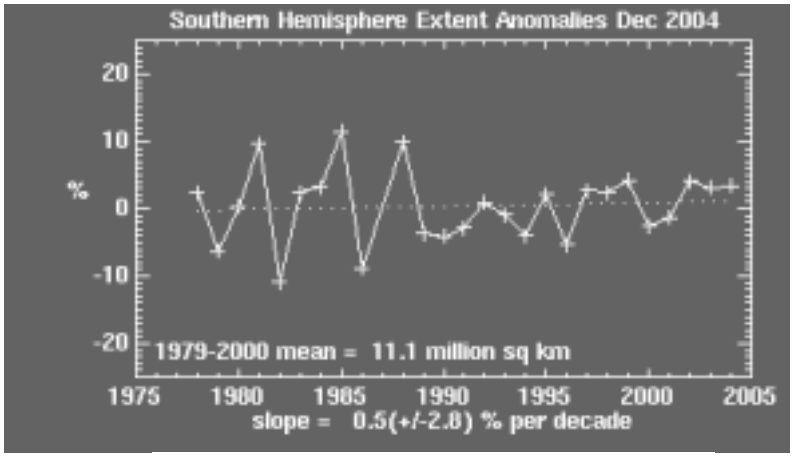

Conc Anomalies
Mar 2004

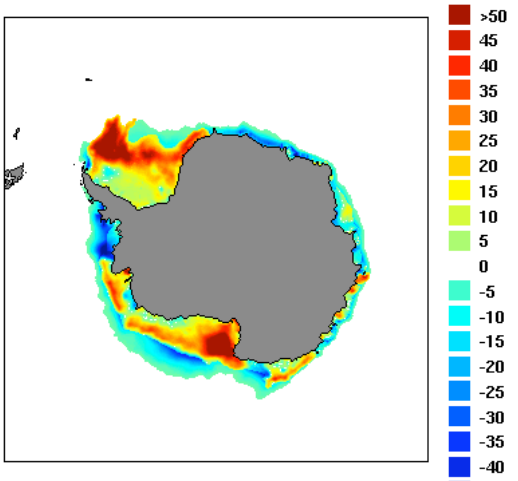

Total anomaly = 0.6 million sq km

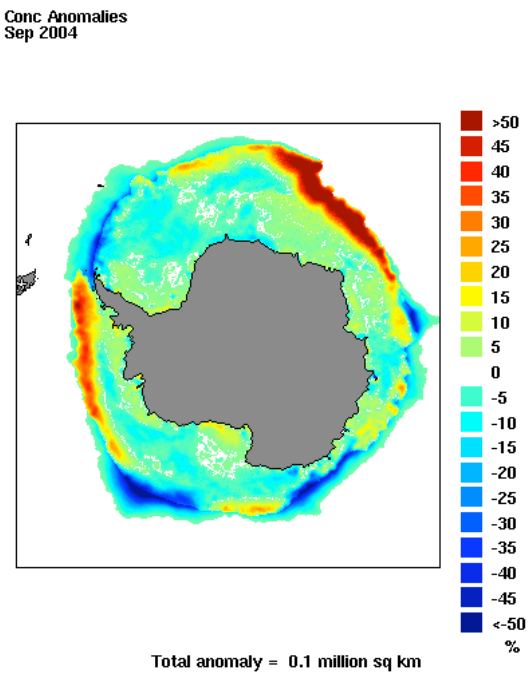

Figure 10. (a) AAO index based on monthly values from the Climate Prediction Center (thick: annual average; medium: JAS average; thin: monthly); (b) Sea ice index (http://nsidc.org/data/seaice_index/) (Fetterer and Knowles 2002, updated 2004); (c) and (d) Ice concentration anomaly in March and September 2004 (http://nsidc.org/data/seaice_index/archives/).

In 2004, the annual average AAO (SAM) was rising. The monthly SST maps (Fig. 1) do not show a simple polar vortex response, instead showing a version of the wavenumber 2 pattern that usually dominates. In the mean in 2004, this pattern included a cold region south of Africa, and a weak cold region in the eastern Ross Sea. Warm patches appeared in the western Ross Sea and Weddell Sea.

In winter (September) 2004, sea ice (Fig. 10d) matched the SST pattern, with increasing sea ice concentration in the cold region south of Africa, and in the eastern South Pacific. The total sea ice cover (Fig. 10b) continued a long-term but very noisy upward trend around Antarctica.

2.3.4.4. North Atlantic Oscillation

The northern North Atlantic (subpolar region and adjacent Nordic Seas, including the Greenland, Iceland and Norwegian Seas) receives special attention because of its role in global overturning circulation and proximity of the affected surface currents to western Europe and the eastern U.S. The overturning culminating in deep and intermediate water formation in the Nordic and Labrador Seas is sometimes called the ocean "conveyor", and is global in extent.

A particular scenario that has received attention is the possibility of freshening of the surface layer of the northern North Atlantic, as a result of ice melt and/or changed precipitation patterns. Such freshening is clearly being observed (section 2.3.5 below). Historically and in models, a freshened surface layer reduces or stops the convection that connects the surface to the intermediate layers in the Greenland and Labrador Seas. Freshwater from the Arctic impacts the Greenland Sea through the East Greenland Current, and impacts the Labrador Sea through Davis Strait.

Northern North Atlantic climate variability is strongly associated with the North Atlantic Oscillation (NAO) and its parent climate pattern, the Arctic Oscillation (AO) or Northern Annular Mode (NAM), which have quasi-decadal time scales. The NAO index measures the meridional atmospheric pressure gradient driving the westerlies. When the NAO index is high, the westerlies are in a northern position and strengthened, and vice versa.

The NAO index in 2004 continued to be close to neutral based on several available products (Fig. 11).

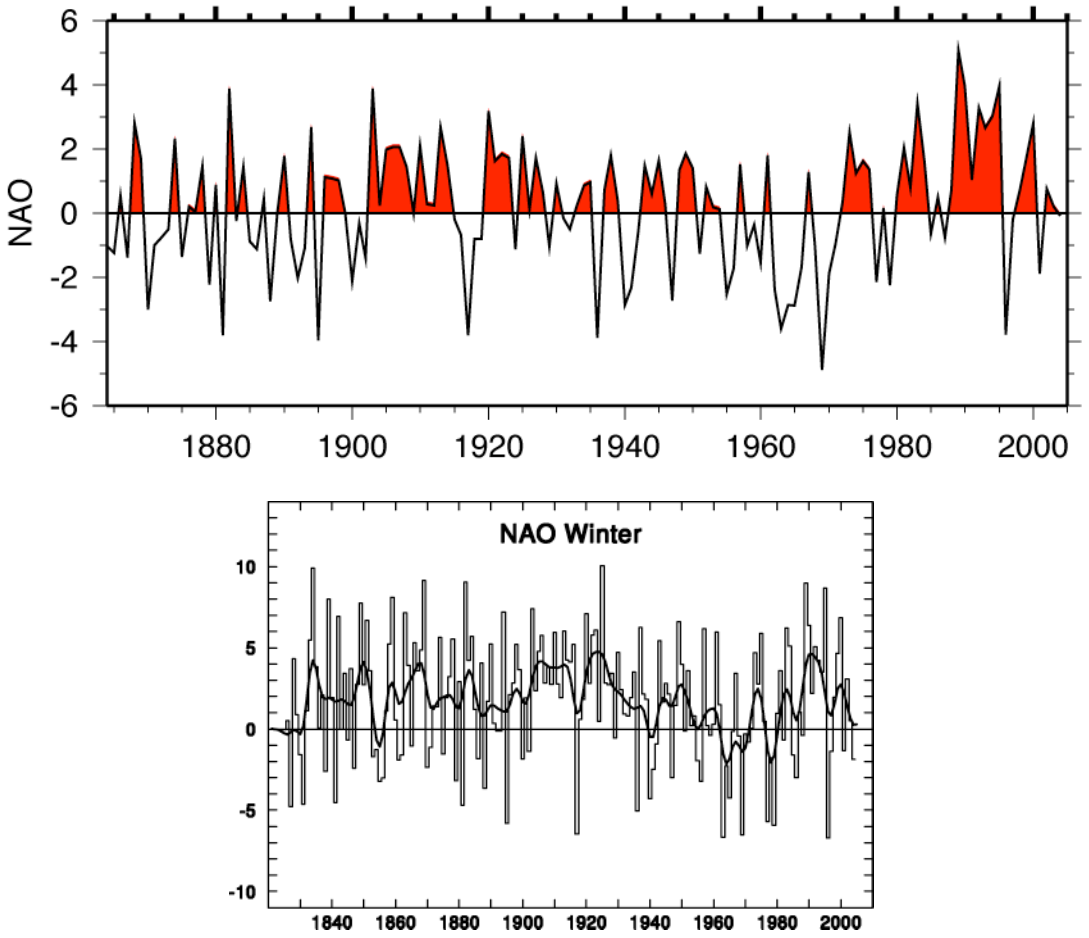

Figure 11. NAO index. (a) Winter Lisbon-Reykjavik SLP difference: values from http://www.cgd.ucar.edu/~jhurrell/nao.stat.winter.html
(b) Gibraltar-Reykjavik pressure difference: image from http://www.cru.uea.ac.uk/cru/climon/data/nao/ (Climate Monitor Online 2005).

Temperature anomalies along the zonal subtropical section crossing the North Atlantic at 24°N show an approximately 20-year signal (Fig. 12).

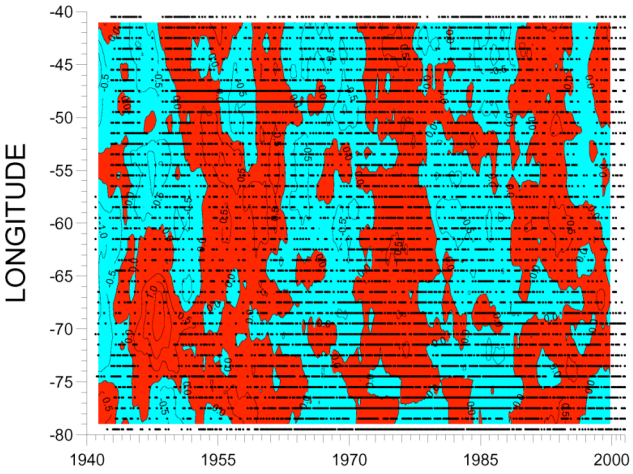

Figure 12. Surface temperature variations from BT and continuing XBT observations along 24°N showing an approximately decadal signal. Annual cycle and long-term trend were removed, and the data were filtered with a 3-year running mean (Baringer/AOML, personal communication).

2.3.5 Global overturning circulation

Deep overturn is affected by surface properties, particularly salinity and the presence and strength of a near-surface halocline. It is also affected by the overall stratification, hence properties, especially salinity, in and below the thermocline. A strong halocline supports surface cooling even to freezing without deep convection, whereas a weak halocline can permit deep overturn. Surface layer salinity is a function of regional precipitation and runoff and export of freshwater from winter ice-covered regions. Changes in freshwater content and sea ice extent thus have impacts on the thermohaline circulation, and are reviewed here.

The two sites that dominate thermohaline circulation of the global ocean are the deep and intermediate water formation sites in the northern North Atlantic, and at sites distributed around Antarctica. The waters from these two regions fill the global ocean, mixing with each other and with overlying thermocline waters. Upwelling occurs in many regions; this component of the thermohaline circulation is not yet well understood, but most likely involves a large amount of upwelling in the tropics and in the southern ocean. The North Pacific participates only weakly in thermohaline circulation because it is relatively fresh compared with the North Atlantic and Antarctic, and is not reviewed herein, although a section could be added on the North Pacific in future reports.

Major changes in thermohaline circulation are associated with glacial-interglacial changes in climate, with paleoclimate observations showing a weakening of the North Atlantic overturning and shift to shallower densities during the glacial periods. Variations in North Atlantic overturning are implicated in models of climate change, especially recent concepts of abrupt climate change (e.g., Alley et al. 2003). Southern Ocean overturning changes are the other end of the variability - models of thermohaline circulation variations often show alternating strength of overturn in the North Atlantic and Southern Ocean, with the implication that the present climate state is of strong North Atlantic overturn and relatively weak Southern Ocean overturn.

Change in thermohaline circulation result from changes in the temperature - salinity distribution and less importantly from changes in air-sea flux. A saltier basin provides the greater and denser

overturn. Changes in the circulation are a response to a buildup over many years, although the actual change is predicted to be quite sudden at some phases of the climate cycle.

2.3.5.1 North Atlantic overturn

The components of North Atlantic Deep Water sink from the surface at convection sites in the Nordic Seas, the Labrador Sea and the Mediterranean Sea. Within the North Atlantic and tropical Atlantic, these three source waters are readily distinguishable. Variations in their properties could be well defined by the completed ARGO network. Future summaries will draw effectively from this source (e.g., Figs. 2 and 3). Current projects that regularly produce subsurface temperature maps do not include the deepest surfaces needed to characterize these water mass changes.

The source water for the sinking in the northern North Atlantic is upper ocean water that enters the North Atlantic from the southern hemisphere and from the Arctic. The Arctic source includes a fresh surface layer associated with continental runoff and the sea ice cycle. Major melting of Arctic sea ice was reported in 2002 and continued in 2003 (Figure 13). These fresh waters are exported to the North Atlantic in the East Greenland Current and through Davis Strait into the Labrador Sea. Freshening of upper ocean waters around the northern North Atlantic has been reported over the past several decades (Dickson et al. 2002, 2004; Curry et al. 2004) (Fig. 16). If continued, the freshening could initiate a weakening of the North Atlantic overturn.

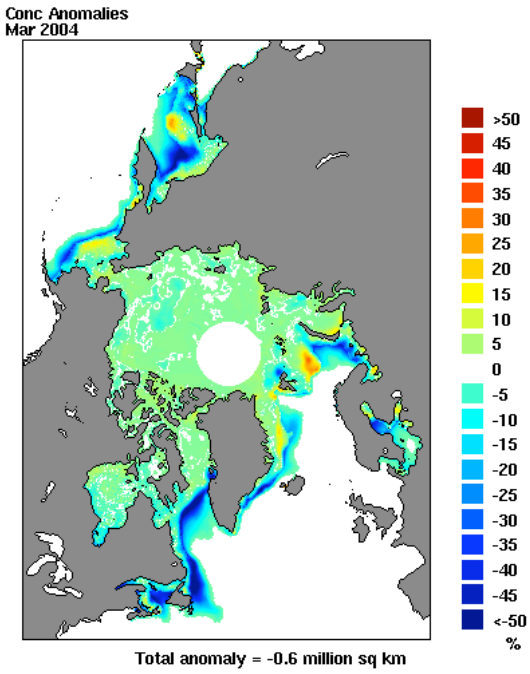

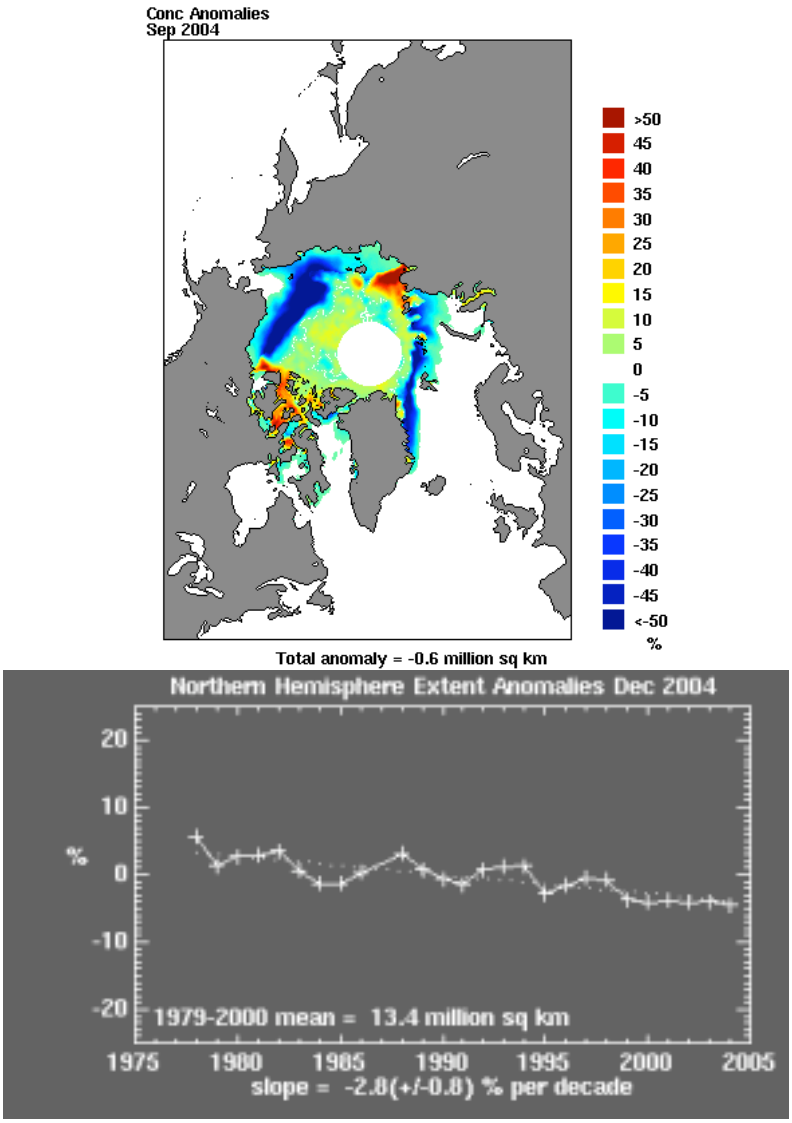

Figure 13. Arctic sea ice: concentration in (a) March 2004 and (b) September 2004. (http://nsidc.org/data/seaice_index/archives/) and (c) Multi-year time series of extent. (http://nsidc.org/data/seaice_index/).

A time series of salinity in the central Labrador Sea shows major freshening of the Labrador Sea Water (very thick near-surface layer) in the mid-1990s associated with vigorous deep convection brought on by high NAO (Fig. 14), continuing in a weaker way to the present. Time series of salinity from various locations around the northern North Atlantic shown by Dickson et al. (2002, 2003) show first the broad spatial scale of freshening. The important freshening trends emerge only with several decades of data and multi-year averaging.

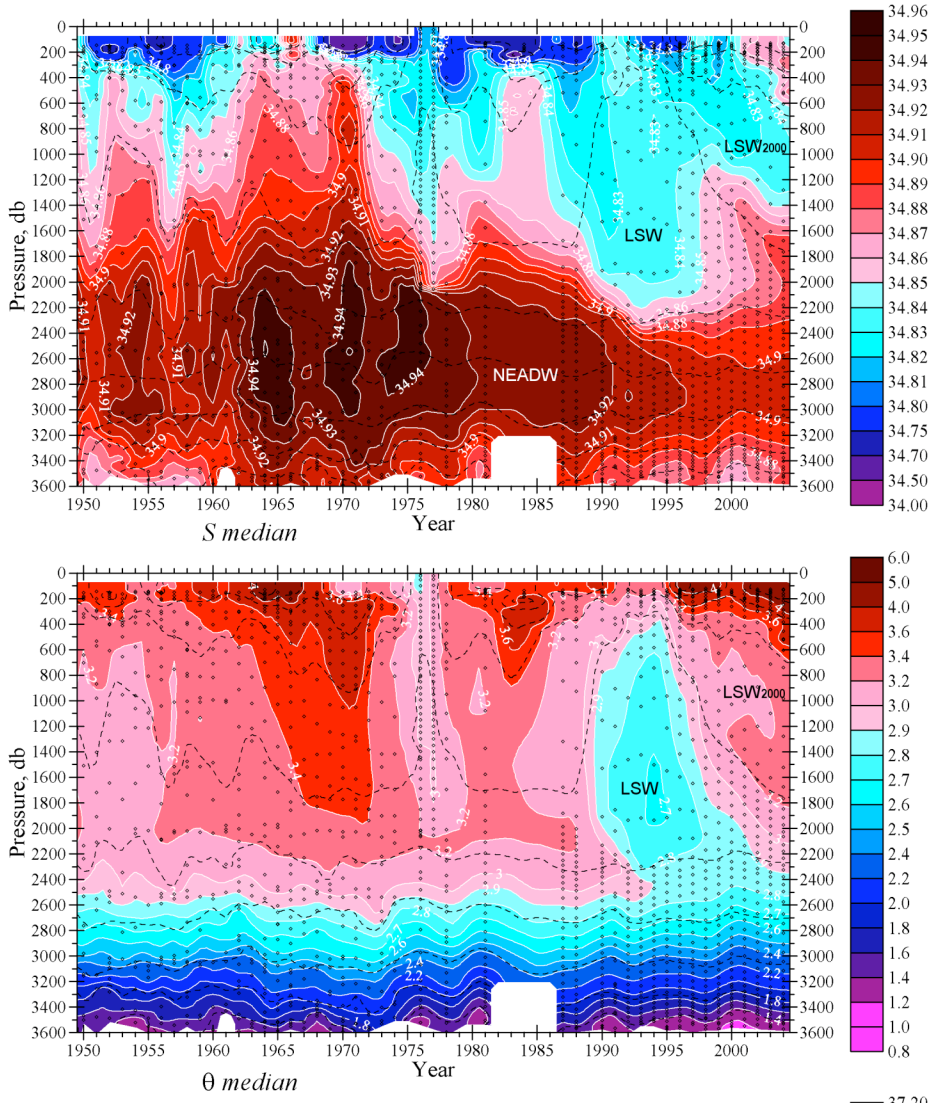

Figure 14. Time series of (a) salinity and (b) potential temperature in the central Labrador Sea. (Yashayaev, personal communication).

The Deep Western Boundary Current (DWBC) in the subtropical North Atlantic carries the various component of the new North Atlantic Deep Water southward. As noted above, these include waters from the Labrador Sea at about 1500-2000 meters and from the Nordic Seas below this. Ongoing observations of the DWBC (Molinari et al. 1998; Baringer personal communication) have shown the arrival of the extreme form of Labrador Sea Water that was formed in the1990s in the Labrador Sea. As of 2002, continuing into 2003, freshening of the whole repeated section crossing the DWBC was apparent.

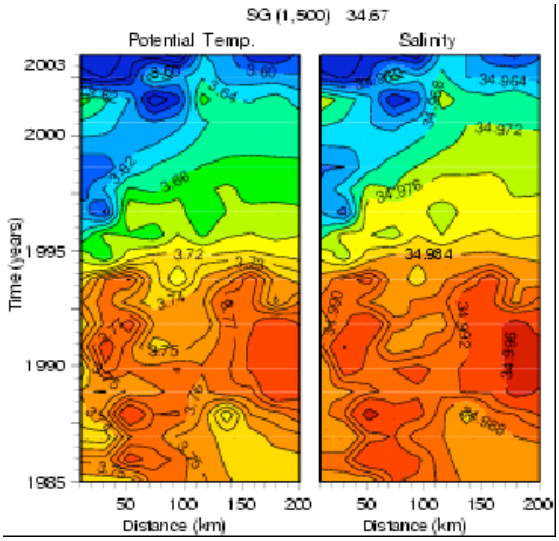

Figure 15. Hydrographic observations crossing the Deep Western Boundary Current east of Abaco at 26.5°N. Shown here are potential temperature and salinity at potential density σ_1= 34.67 (depth ~ 1500-1700 meters), showing the arrival of cold, fresh Labrador Sea Water after 1995 (from M. Baringer, NOAA/AOML).

Overall, the Atlantic has been becoming fresher and colder at high latitudes and more saline and warmer in subtropical latitudes (Curry et al. 2004) (Fig. 16). This suggests an increase in the strength of the hydrological cycle. The high latitude freshening could impact dense water formation adversely.

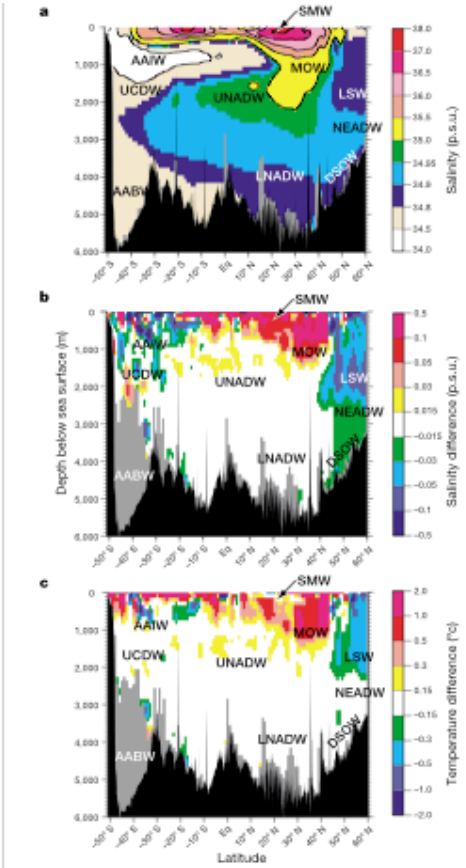

Figure 16. Changes in salinity and temperature of the major water masses in the Atlantic Ocean, along a section from south to north (Curry et al. 2004).

2.3.5.2. Southern Ocean overturn

Bottom waters are formed around Antarctica through brine rejection in polynyas near the coast. Deep waters are formed by deep convection in the Weddell and Ross Seas. The global overturning circulation also has an important upward limb in the Circumpolar Current system located north of the winter ice edge northward through the Subantarctic Front, where deep waters, formed in the North Atlantic and modified in the deep Indian and deep Pacific Oceans, upwell.

Sea ice extent around Antarctica in 2004 was illustrated in section 2.3.4.3 and in Figure 10. The densest waters in the world are formed in polynyas in the coastal regions of Antarctica, over the continental shelves. With increasing sea ice production, as has been occurring in the Antarctic over the past several decades (noisy increase seen in Fig. 10), denser shelf waters and hence denser bottom waters can be formed. With a decrease in summer ice melt (or smaller contrast between winter and summer ice extent), the freshwater surface layer inhibiting surface mixing would weaken, which also increases density and production of dense waters. Thus the changing sea ice conditions around Antarctica would appear to favor an increase in dense water production and density.

Variations in upper ocean temperature and salinity in the Australian sector of the Southern Ocean (Aoki et al. submitted) (Fig. 17) bear out this potential for increased dense water production. The surface waters in the south are becoming more saline while those at subtropical latitudes are becoming fresher. The increased salinity in the south could allow higher density convection.

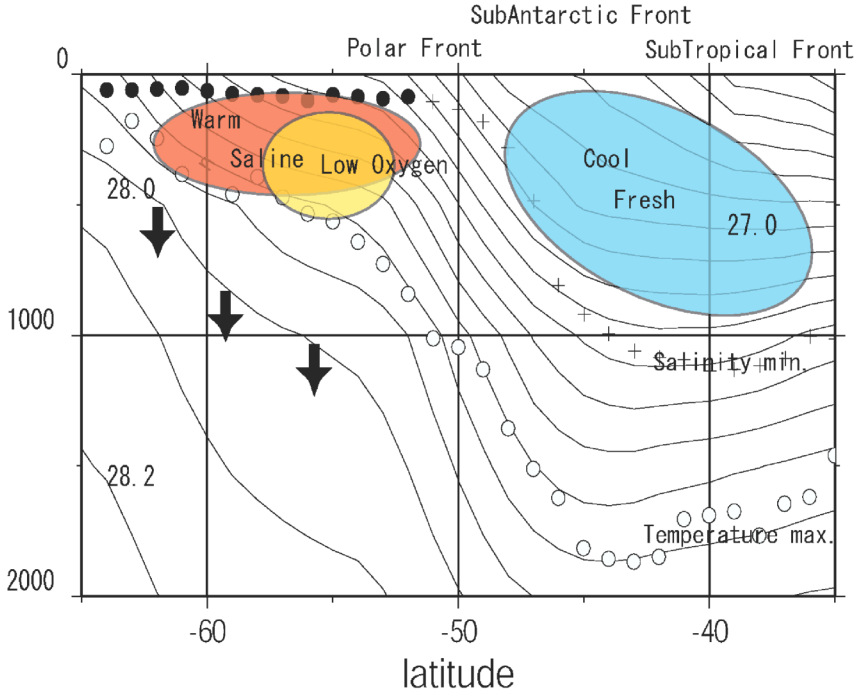

Figure 17. A summary of the meridional water mass changes from south of the ACC to mid-latitudes, between 30E and 160E (Aoki et al. 2005).

2.3.6. Heat and freshwater transport variations based on *in situ* data

Ocean heat and freshwater transports are calculated from either their air-sea fluxes or directly from in situ ocean observations of temperature, salinity and velocity. Annual global and full water column data sets of *in situ* properties, with requisite velocity analysis, are not possible.

Willis et al. (2004) have pioneered a mapping of ocean heat content from a combination of in situ measurements (ARGO and XBT profiles), altimetric sea surface height, and data assimilation. Using data through mid-2003, they show that the global heat content of the ocean has been rising since 1993 (onset of altimetry observations) (Fig. 18). Their analysis excludes the Arctic and southern ocean, and so the actual rise is likely larger, given the much larger SST increases observed in the Arctic than in the mid-latitude oceans (Fig. 1 and section 2.3.3).

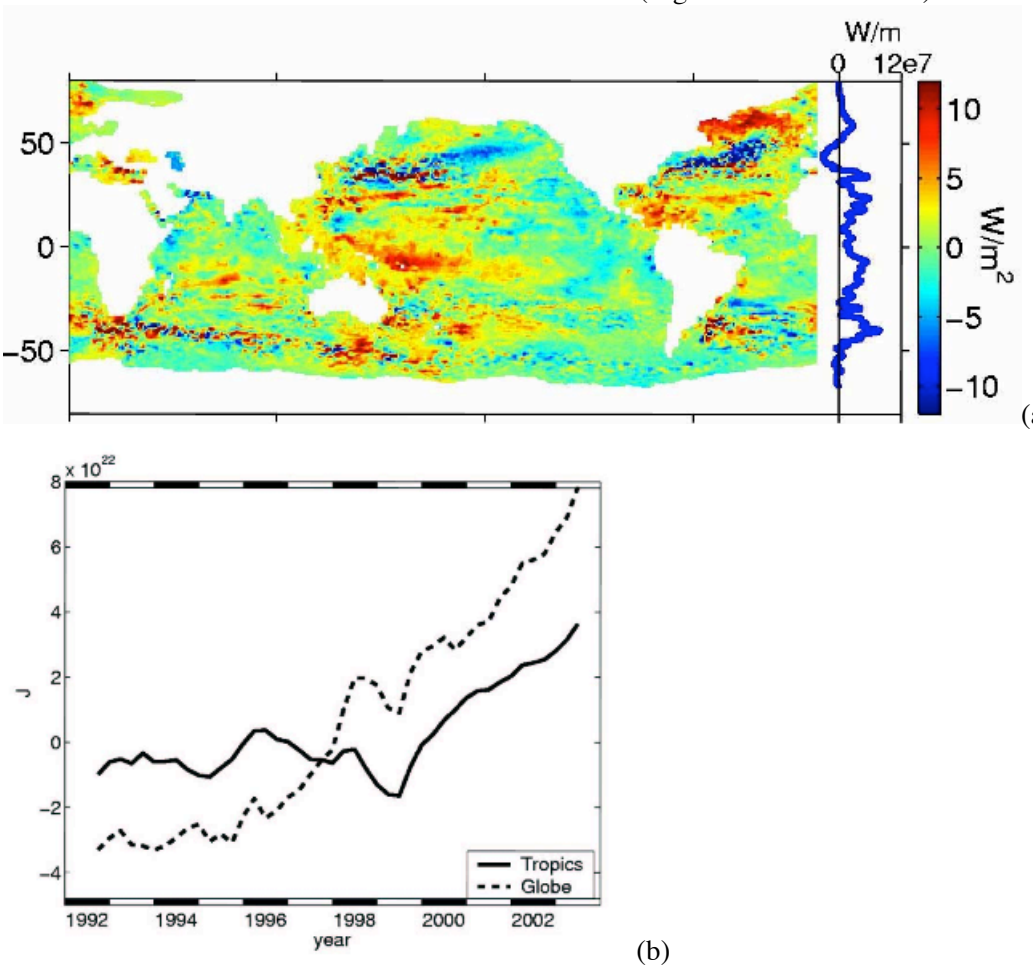

Figure 18. Ocean heat content: (a) mapped changes from 1993 to 2003 in terms of surface heat flux (W/m^2), and (b) total heat content (Joules) integrated over the globe (Willis et al. 2004).

References

Aoki S., N.L. Bindoff, and J.A. Church: Interdecadal Water-mass changes in the Southern Ocean between 30E and 160E. *Geophys. Res. Lett.*, to be submitted.

Curry R., B. Dickson, and I. Yashayaev, 2004: A change in the freshwater balance of the Atlantic Ocean over the past four decades. *Nature*, **426**, 826-829.

Dickson, R. R., R. Curry and I. Yashayaev, 2003: Recent changes in the North Atlantic. *Phil. Trans. Roy. Soc.*, London A, 10.1098/rsta.2003. **1237**, 18 pp.

Fetterer, F. and K. Knowles. 2002, updated 2004: Sea Ice Index. Boulder, CO: National Snow and Ice Data Center. Digital media.

Mantua, N.J., S. R. Hare, Y. Zhang, J. M. Wallace and R. C. Francis, 1997: A Pacific interdecadal climate oscillation with impacts on salmon production. *Bull. Amer. Meteor. Soc.,* **78**, 1069-1079.

Reynolds, R. W., N. A. Rayner, T. M. Smith, D. C. Stokes and W. Wang, 2002: An improved in situ and satellite SST analysis for climate. *J. Climate*, **15**, 1609-1625.

Saji, N. H., N. Goswami, P. N. Vinayachandran and T. Yamagata, 1999: A dipole mode in the tropical Indian Ocean. *Nature*, **401**, 360-363.

Smith, T. M. and R. W. Reynolds, 2003: Extended Reconstruction of Global Sea Surface Temperatures Based on COADS Data (1854-1997). *J. Climate*, **16**, 1495-1510.

Thompson, DWJ, and JM Wallace, 2000: Annular modes in the extratropical circulation. Part I: Month-to-month variability. *J. Climate*, **13**, 1000-1016.

Willey, D. A., R. A. Fine, R. E. Sonnerup, J. L. Bullister, W. M Smethie and M. J. Warner, 2004. Global oceanic chlorofluorocarbon inventory. *Geophys. Res. Lett.,* **31**, L01303, doi:10.1029/2003GL018816.

Willis, J. K., D. Roemmich and B. Cornuelle, 2004: Interannual variability in upper ocean heat content, temperature, and thermosteric expansion on global scales. *J. Geophys. Res.*, **109**, C12036, doi:10.1029/2003JC002260.

Wunsch, C. 2002: What is the thermohaline circulation? *Science*, **298**, 1179-1181.

Zhang, Y., J.M. Wallace, D.S. Battisti, 1997: ENSO-like interdecadal variability: 1900-93. *J. Climate*, **10**, 1004-1020.

2.4 EVOLUTION OF THE 2004 EL NIÑO

by Michael J. McPhaden, Pacific Marine Environmental Laboratory, Seattle, Washington

A weak El Niño developed in the second half of 2004 in the equatorial Pacific. Anomalous warming was for the most part centered around the international date line, with near normal temperatures in the equatorial cold tongue of the eastern Pacific and along the west coast of South America. SST anomalies in the NINO3.4 index region (5°N-5°S, 120°-170°W) were approximately 0.8°C on average from August to December 2004. The Southern Oscillation Index (SOI), which is the normalized surface air pressure difference between Darwin, Australia and Tahiti, French Polynesia, was consistently negative during the latter half of 2004 (-0.6 on average for August-December) indicative of warm phase El Niño/Southern Oscilllation (ENSO) conditions. The trade winds were unusually weak west of the date line associated with the elevated central and western Pacific SSTs and negative SOI values. Conversely, trade winds in the eastern Pacific were near to or even slightly stronger than normal throughout much of 2004.

The 2004 El Niño was characterized by significant month-to-month variability, much of which was associated with the atmospheric Madden-Julian Oscillation (MJO). Individual MJO events were initiated by convective flare-ups over the Indian Ocean and subsequently propagated eastward into the western Pacific. The westerly phase of the MJO was linked to 2-3 week long westerly wind bursts in the western Pacific, which forced eastward propagating downwelling intraseasonal equatorial Kelvin waves (Fig. 1). These waves deepened the thermocline in the eastern Pacific by 20-30 m, but apparently had little impact on eastern Pacific SSTs.

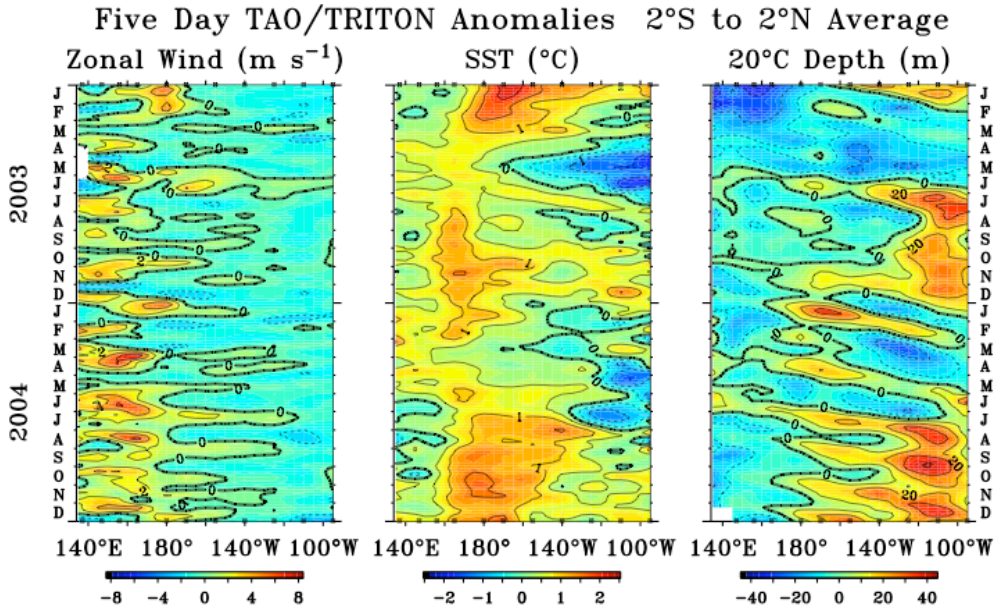

Figure 1. Five-day average anomalies of zonal wind, SST, and 20°C depth (an index for the depth of the thermocline) relative to the mean seasonal cycle averaged 2°N–2°S based on TAO/TRITON moored time series data. Ticks on the horizontal axis indicate longitudes sampled at the start (top) and end (bottom) of record.

Intraseasonal variability in convection was also pronounced in the western Pacific, but persistent anomalous atmospheric convection failed to develop over the elevated SSTs near the date line during the latter half of 2004. Thus, the ocean and the atmosphere did not appear to be as

strongly coupled as in previous El Niño events. Lack of persistent anomalous deep convection in the western and central Pacific limited the impact of the El Niño on the global atmospheric circulation and teleconnections to higher latitudes in 2004. Likewise, the failure of persistent El Niño-related warm SST anomalies to develop in the eastern equatorial Pacific and along the west coasts of the Americas limited the effects of this El Niño on marine ecosystems and commercial fisheries in those regions.

The 2004 El Niño was unusual in that it followed the moderate amplitude 2002-03 El Niño (McPhaden 2004) by only one year. This rapid sequencing of El Niños is analogous to what transpired in the early 1990s when the moderate amplitude 1991-92 El Niño was followed by a weak warm event in 1993. Factors contributing to the development of the 2004 El Niño so soon after the termination of the previous event are not fully understood. However, it is noteworthy that the 2002-03 El Niño was followed by an extended period of excess warm water volume (or equivalently heat content) in the equatorial zone, which is atypical of conditions following most El Niños (Fig. 2). According to the recharge oscillator theory for ENSO (Jin 1997), El Niño is supposed to purge the tropical Pacific of excess heat leaving a deficit that must be replenished before the next El Niño can occur. The presence of weak positive heat content anomalies following the 2002-03 El Niño created large-scale conditions favorable the recurrence of another warm event earlier than would otherwise have been expected. Episodic westerly wind forcing in boreal spring and summer 2004 (Fig. 1) may have served as the stimulus for the development of anomalous warming by displacing the western Pacific warm pool towards the east (Kessler et al. 1995).

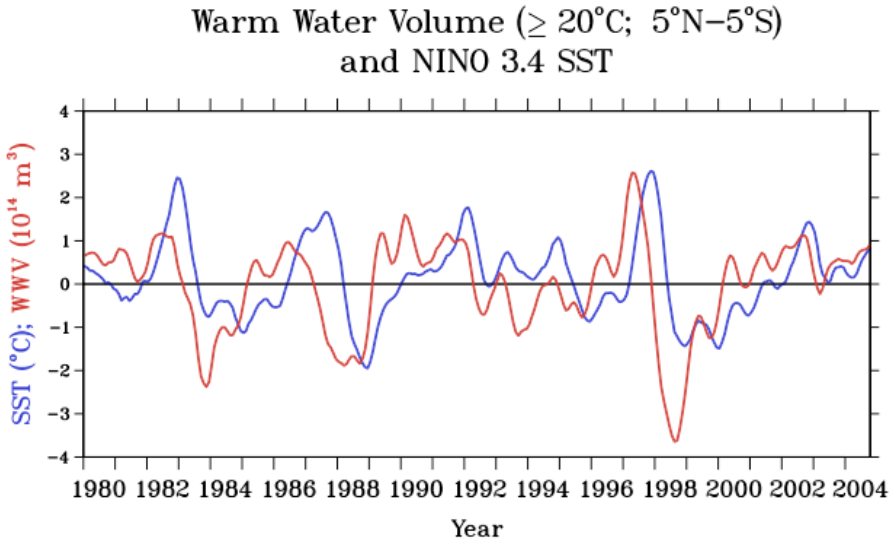

Figure 2. Monthly anomalies of warm water volume (5°N–5°S, 80°W–120°E above the 20°C isotherm) and NINO3.4 SST (5°N–5°S, 120°W–170°W) from January 1980 to December 2004. Warm water volume is based on a blended analysis of TAO/TRITON moored time series data and ship-of-opportunity expendable bathythermograph (XBT) data. Time series have been smoothed with a 5-month running mean filter for display.

Another unusual feature of the 2004 El Niño was the concentration of warm equatorial SST anomalies near the date line. A similar pattern was evident during the 2002-03 El Niño (see for example the start of the SST anomaly time series in Figure 1). In contrast, for most previous El Niños, eastern Pacific SST anomalies were much more pronounced. It is unclear what factors were responsible for this SST anomaly pattern. One possibility is that the Pacific has gone

through a decadal regime shift in the late 1990s towards stronger trades and colder cold tongue SSTs (McPhaden and Zhang 2004). Such a decadal change in background state could favor weaker cold tongue SSTs during El Niño, but other processes may be at work as well.

Statistical and dynamical ENSO forecast models suggest that El Niño conditions will persist through the boreal spring of 2005 (http://iri.ldeo.columbia.edu/pred/). Afterwards, the models indicate a general tendency for continued warm SST anomalies with only slightly diminished amplitudes. However, forecasts through the "spring predictability barrier" are generally less reliable than those made up to and including the spring season, so there is greater uncertainty in El Niño forecasts for mid-2005 and beyond.

References

Jin, F.F., 1997: An equatorial recharge paradigm for ENSO. Part I: Conceptual model. *J. Atmos. Sci.*, **54**, 811-829.

Kessler, W.S., M.J. McPhaden, and K.M. Weickmann, 1995: Forcing of intraseasonal Kelvin Waves in the equatorial Pacific. *J. Geophys. Res.*, **100**, 10,613-10,631.

McPhaden, M.J., 2004: Evolution of the 2002-03 El Niño. *Bull. Am. Meteorol. Soc.*, **85**, 677-695.

McPhaden, M.J. and D. Zhang, 2004: Pacific Ocean circulation rebounds. *Geophys. Res. Lett.*, **31**, L18301, doi:10.1029/2004GL020727.

2.5 THE GLOBAL OCEAN CARBON CYCLE: INVENTORIES, SOURCES AND SINKS

by Richard Feely[1] and Rik Wanninkhof[2]

[1]Pacific Marine Environmental Laboratory, Seattle, Washington
[2]Atlantic Oceanographic and Meteorological Laboratory, Miami, Florida

Abstract
The ocean plays a major role in the global carbon cycle as it is a vast reservoir of carbon, naturally exchanges carbon with the atmosphere, and consequently takes up a substantial portion of anthropogenic carbon from the atmosphere. In response to the need for an integrated investigation of the carbon cycle in the oceans, the CLIVAR/CO_2 Repeat Hydrography and NOAA Underway pCO_2 Measurements Programs were established to document the trends in carbon uptake and transport in the global oceans. The CLIVAR/CO_2 Repeat Hydrography Program consists of a systematic re-occupation of select hydrographic sections to quantify global changes in storage and transport of heat, fresh water, carbon dioxide (CO_2), chlorofluorocarbon tracers and related parameters. Three North Atlantic cruises in 2003 marked the beginning of the US effort by reoccupying selected hydrographic sections on decadal time-scales. Early results from these cruises showed significant changes in oxygen and carbon dioxide and several other measurable parameters since the last global survey in the 1990s. The increases of DIC in the Subtropical Mode waters (STMW) are greater than expected from invasion of anthropogenic CO_2 from the atmosphere and may be the result of decadal changes in the local circulation in the North Atlantic.

2.5.1 The Global Carbon Cycle: Inventories, Sources and Sinks

The global utilization of fossil fuels for energy by mankind is rapidly changing the trace gas composition of the Earth's atmosphere, causing the greenhouse warming from excess CO_2 along with other trace gas species such as water vapor, chlorofluorocarbons (CFCs), methane, and nitrous oxide. These anthropogenic "greenhouse gases" play a critical role in controlling the earth's climate because they increase the infrared opacity of the atmosphere, causing the planetary surface to warm. Carbon dioxide is one of the major greenhouse gases, contributing about 60% of the total change in radiative forcing due to human perturbations. The release of CO_2 from fossil fuels and deforestation processes contributes approximately 6.3 ± 0.4 Pg C per year (Sabine et al. 2004a) to the atmosphere. Of this amount, approximately 3 Pg C of this so-called "anthropogenic CO_2" accumulates in the atmosphere and causes the atmospheric CO_2 levels to increase. The remaining 4 Pg C is sequestered by the terrestrial biosphere and global oceans. Where and how these two major sink regions vary in their uptake of CO_2 from year to year is the subject of much scientific research (Houghton et al. 2001).

The ocean plays a major role in the global carbon cycle as it is a vast reservoir of carbon, naturally exchanges carbon with the atmosphere, and consequently takes up a substantial portion of anthropogenic carbon from the atmosphere. Current estimates of anthropogenic CO_2 uptake by the oceans in the 1990s are about 1.9 ± 0.7 Pg C yr^{-1} (Figure 1; Sabine et al. 2004a). Future decisions on regulating emissions of greenhouse gases should be based on more accurate models of CO_2 sources and sinks that have been adequately tested against a well-designed system of measurements. The construction of a believable present-day carbon budget is essential for the reliable prediction of atmospheric CO_2 and global temperatures from available emission scenarios.

Our current understanding of the fate of the anthropogenic CO_2 released to the atmosphere is based on models; atmospheric observations of CO_2, carbon isotopes and small decreases in

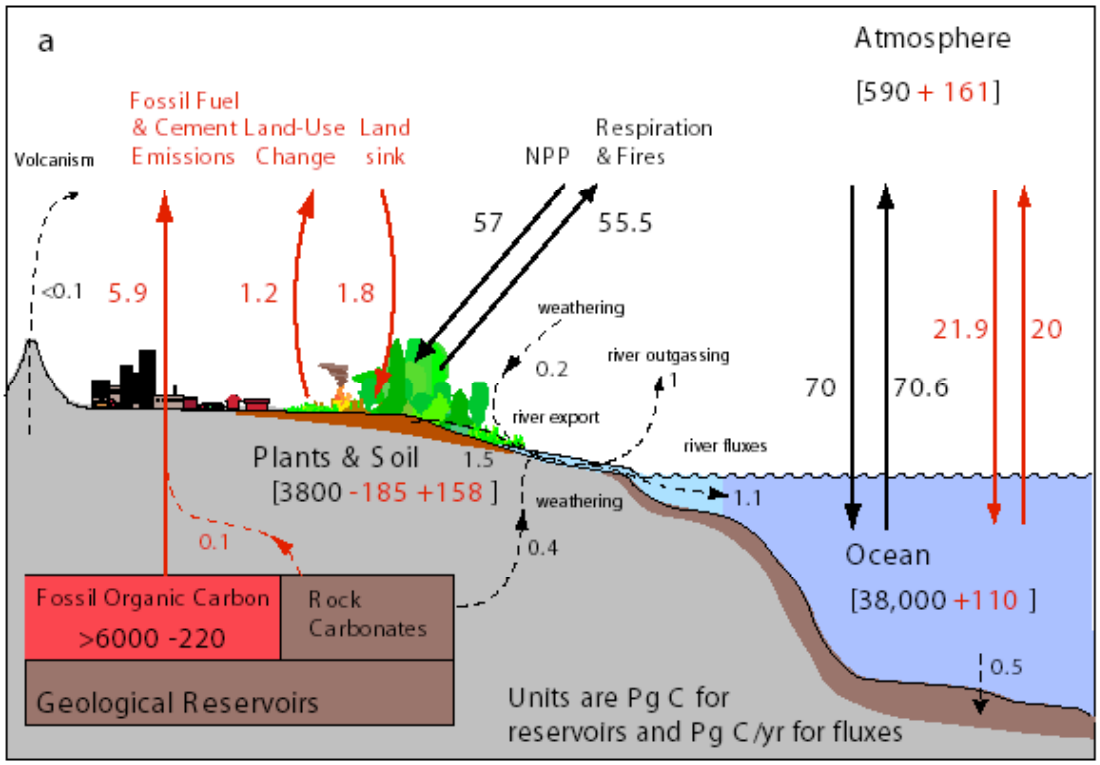

Figure 1. Cartoon of fluxes (arrows) and inventories (number in boxes) of the labile components of the global carbon system for the 1980ties. The red arrows are the perturbation fluxes resulting from emissions of anthropogenic CO_2 (Sabine et al. 2004a).

oxygen levels; terrestrial measurement of biomass inventories and primary productivity; and oceanic measurements of CO_2 inventories and fluxes between air and ocean. Less than a decade ago there were significant discrepancies between estimates leading to the popular notion of the "missing carbon sink" there now is a broad agreement that the "missing sink" is uptake by the terrestrial ecosystems based on disparate methods as summarized in Table 1. As the table indicates, our level of confidence in different observations ranges from a general good knowledge of the annual changes in some reservoirs, to highly uncertain estimates in others. Annual releases due to fossil fuel burning and cement production, and annual atmospheric CO_2 increases are the most constrained. Decadal changes in the ocean carbon inventory have recently been established with reasonable confidence. Changes in the terrestrial biosphere have been more difficult to pinpoint. From a variety of observations we now have a reasonable estimate of the partitioning of the fossil fuel carbon between reservoirs over the last two centuries with roughly 50% ending up in the ocean. The terrestrial systems released CO_2 over this same period. Over the last two decades, however, the terrestrial systems appear to have taken up CO_2 but the magnitude, cause, and particularly the longevity of this sink remains in great doubt. Significant efforts, such as those proposed in the North American Carbon Plan (NACP), are underway to directly determine CO_2 sources and sinks in the terrestrial system. However, in the foreseeable future the best approach for constraining the net terrestrial flux will be from the difference between atmospheric and oceanic observations and model calculations.

Table 1. Global inventory of anthropogenic CO_2 for the past 200 and 20 years

CO_2 Sources	1800-1994 [Pg C][a]		1980-1999 [Pg C][g]
Constrained sources and sinks			
(1) Emissions from fossil fuel and cement production	244 [(b)]	± 20	117±5
(2) Storage in the atmosphere	-165 [(c)]	± 4	-65±1
(3) Uptake and storage in the ocean	-118 [(d)]	± 19	-37±8
Inferred net terrestrial balance			
(4) Net terrestrial balance = [-(1)-(2)-(3)]	39	± 28	-15±9
Terrestrial balance			
(5) Emissions from land use change	100 to180[(e)]		24±12
(6) Terrestrial biosphere sink = [-(1)-(2)-(3)]-(5)	-61 to -141		-39±18

(From Sabine et al. 2004a)

The need for an integrated investigation of the carbon cycle has been well articulated in the US Carbon Cycle Science Plan (Sarmiento and Wofsy 1999). Through efforts of the Interagency Carbon Working Group and the Scientific Advisory Committee, science and implementation plans have been developed for subcomponents of the program including the NACP Science Plan, the NACP Implementation Strategy, the Ocean Carbon and Climate Change Implementation Strategy, and the Large Scale Carbon Observing Plan (LSCOP) (Bender et al. 2002). The LSCOP plan in particular focuses on the implementation and justification for sustained ocean observations. All of the plans address the central tenets of the Carbon Cycle Science Plan, which focuses on the "excess carbon", that is the carbon produced by fossil fuel burning and other activities of mankind releasing CO_2 such as land use change:

- Where has the excess carbon gone to over the last two centuries?
- Where will the excess carbon go to in the future?
- What processes are involved in sequestration of the excess carbon?
- Can the future sinks be managed and increased?

Because of the sensitivity of the global economy to terrestrial and oceanic ecosystems, and regional climate, the issue of carbon accounting transgresses the usual stakeholders of scientific information. Like emissions of pollutants, carbon emissions now have an economic value. A number $40 per metric ton carbon sequestered is often used in estimates. Improved constraints on the carbon sources and sinks can now be directly translated into a currency equivalent. For

instance the global uptake of carbon by the ocean of about 1.6 Pg C yr^{-1} (Table 2) translates into a $64 billion service to the global economy. As shown in Table 2, the uncertainty in the ocean sink is significant translating into an uncertainty in the value of this commodity. Knowledge of the future sink strength of the ocean is thus a critical from scientific and economic perspective.

Table 2
Summary of estimated global CO_2 fluxes using different gas transfer velocities but the same ΔpCO_2 climatology

Parameterization	Uptake (Pg C/yr)
Wanninkhof, 1992	-1.6
Wanninkhof&McGillis, 1999	-1.9
Nightingale, 2000	-1.2
Liss and Merlivat, 1983	-1.0

All these values were obtained using the ΔpCO_2 climatology of Takahashi et al. 2002 and 41-year climatological 6-hour winds from the NCAR/NCEP reanalysis project. The divergence of values illustrates that besides determining seasonal ΔpCO_2 fields the gas transfer velocity needs to be better constrained.

The Sustained Ocean Component of the Carbon Cycle Science Plan The oceanic carbon-observing program addresses two important subcomponents of the determination of the fate of the excess CO_2 in the ocean:

- Determining oceanic carbon inventories and attributing the cause of the variations in inventories over time
- Quantifying the air-sea CO_2 fluxes and creating of seasonal flux maps

Ocean inventories
As a result of the measurements during the global CO_2 survey in the 1990s and improved methods of quantifying the anthropogenic CO_2 signal above the large natural background, we now have the first measurement based inventory of anthropogenic CO_2 in the ocean (Fig. 2). The excess CO_2 has been gridded at 1 degree spacing and 33 levels so it can be compared directly with model outputs. Anthropogenic CO_2 is unevenly distributed throughout the oceans. The highest vertically integrated concentrations are found in the North Atlantic, leading this ocean basin to store 23% of the global oceanic anthropogenic CO_2, despite covering only 15% of the global ocean area. The Southern Ocean south of 50ºS has very low vertically integrated anthropogenic CO_2 concentrations, containing only 9% of the global inventory. Approximately 60% of the total oceanic anthropogenic CO_2 inventory is stored in the Southern Hemisphere oceans, roughly in proportion to the larger ocean area of this hemisphere. Characteristic cross sections for the Atlantic, Indian and Pacific basins are shown in Figure 3. The distribution closely follows the known ventilation pathways of the ocean with deep penetration in the North Atlantic and storage of much of the carbon in the mid-latitude convergence zones. The total uptake over the past 200 years shown in Table 1 validates the model estimates. The total inventory is similar to models but the regional inventory is quite different suggesting that most of the models do not adequately capture the processes responsible for uptake at regional scales.

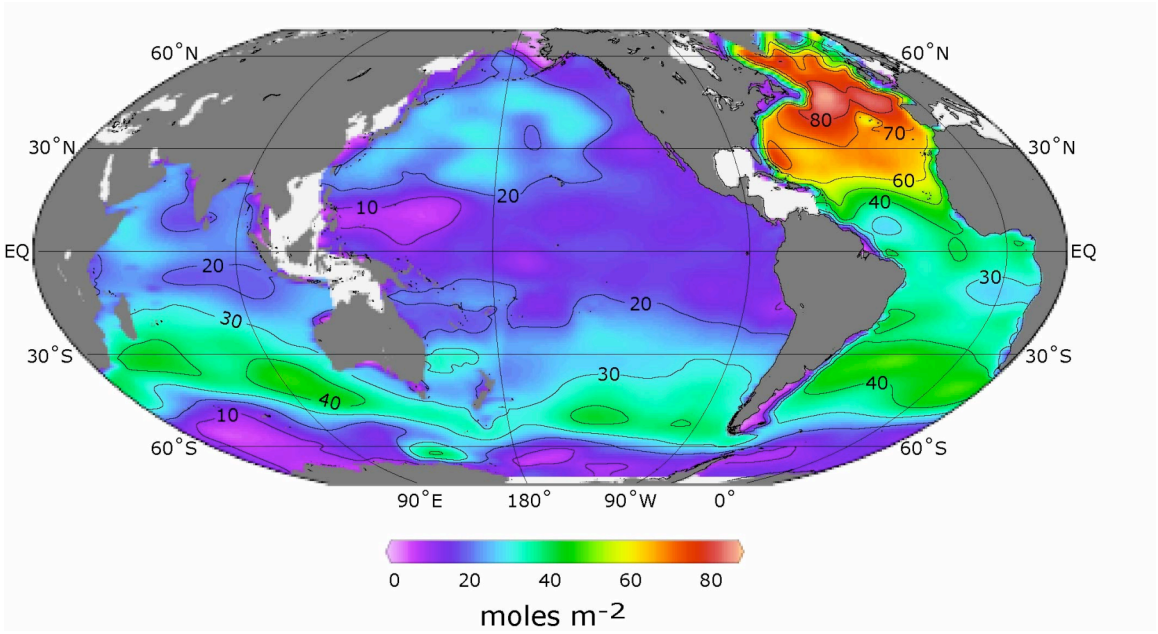

Figure 2. Column inventory of anthropogenic CO_2 in the ocean. High inventories are associated with Deep Water formation in the North Atlantic and Intermediate and Mode Water formation between 30°-50°S. Total inventory of shaded regions is 106±17 Pg C (after Sabine et al. 2004b).

Approximately 30% of the anthropogenic CO_2 is found shallower than 200 m and nearly 50% above 400 m depth (Fig. 3). The global average depth of the 5μmol kg^{-1} contour is approximately 1000 m. The majority of the anthropogenic CO_2 in the ocean is, therefore, confined to the thermocline, i.e., the region of the upper ocean, where temperature changes rapidly with depth. The deepest penetrations are associated with convergence zones at temperate latitudes where water that has recently been in contact with the atmosphere can be transported into the ocean interior. Low vertical penetration is generally observed in regions of upwelling, such as the Equatorial Pacific, where intermediate depth waters, low in anthropogenic CO_2, are transported toward the surface.

Decadal inventory changes

The measurement based total inventory of anthropogenic carbon in the ocean is a critical constraint for models and for our understanding of the role of the ocean in the sequestration of excess carbon. However, information on shorter timescales is essential to determine any feedbacks of oceanic carbon sequestration due to climate change, and to determine the role of natural variability on the oceanic carbon system. Therefore the COSP has started, in collaboration with NSF and NASA, a CLIVAR/CO_2 Repeat Hydrography Program. The main objective of the repeat hydrography component of the sustained ocean observing system for climate is to document long-term trends in carbon storage and transport in the global oceans. This program will provide composite global ocean observing system large-scale observations that include: 1) detailed basin-wide observations of CO_2, hydrography, and tracer measurements; and 2) data delivery and management. This repeat hydrography program will provide the critical and timely information needed for climate research and assessments, as well as long-term, climate quality, and global data sets.

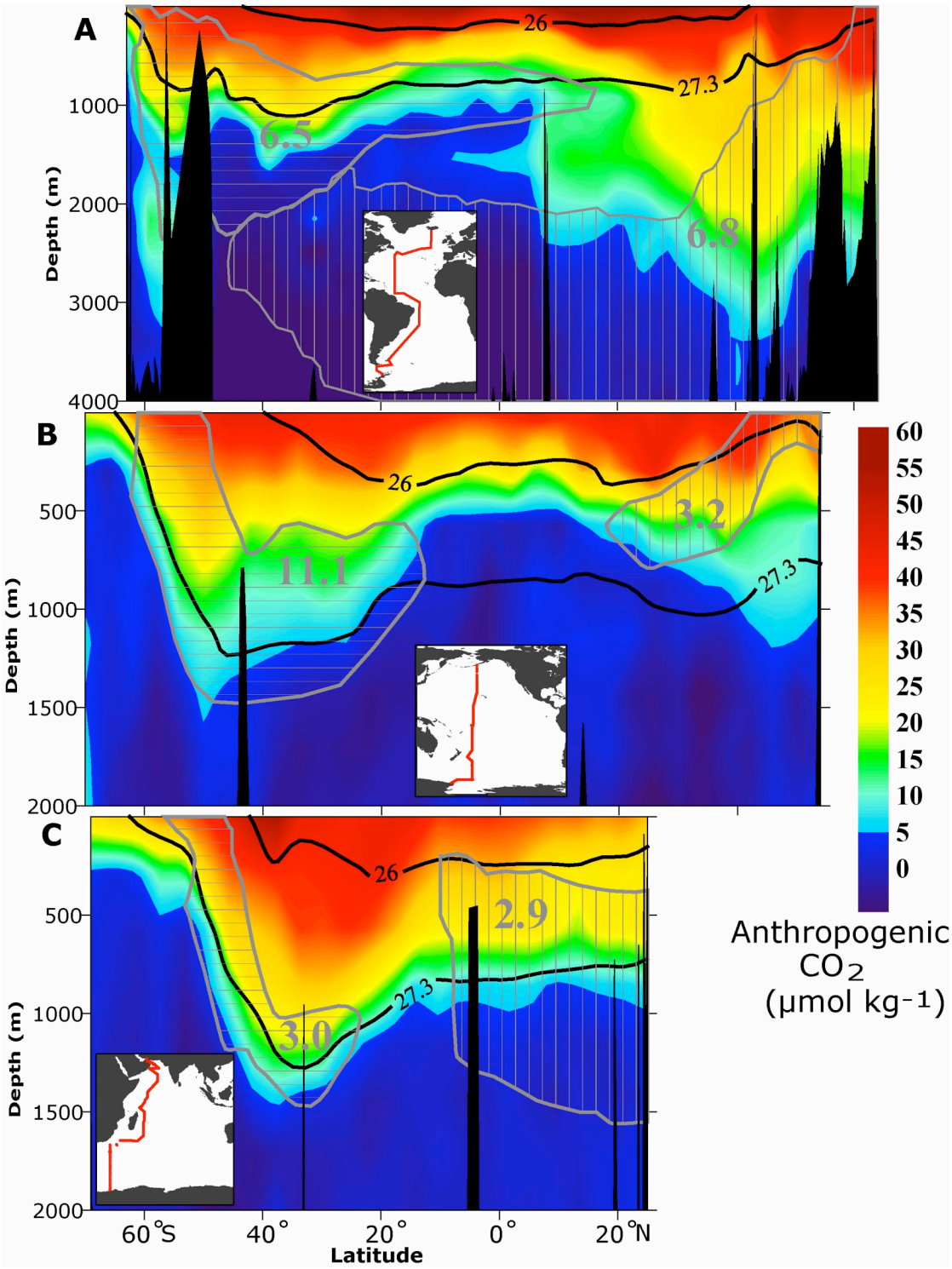

Figure 3. Representative sections of anthropogenic CO_2 (μmol kg^{-1}) from the Atlantic (a), Pacific (b) and Indian (c) oceans. Grey hatched regions and numbers indicate amount of anthropogenic carbon stored (Pg C) in the intermediate water masses The two heavy lines on each section give the characteristic potential density contours for the near surface water and intermediate water. Much of the penetration of anthropogenic carbon into the ocean follow isopycnal surfaces. From Sabine et al. 2004b.

The first three cruises of the Repeat Hydrography Program in 2003 marked the beginning of a large effort to document long-term trends in carbon storage and transport in the global oceans by reoccupying selected hydrographic sections on decadal time-scales. Early results from this work showed significant changes in oxygen and carbon dioxide and several other measurable parameters since the last global survey in the 1990s.

The initial highlights are that the ventilation pattern/circulation in the North Atlantic thermocline has changed based on a significant change in oxygen content. Also, we have been able to unambiguously determine an increase in total carbon content in the upper ocean over 6 to 10 years suggesting that uptake of anthropogenic CO_2 continues unabated and that we can detect anthropogenic carbon increase in the ocean on decadal timescales (Fig. 4). The data indicate significant increases of DIC in the shallow waters masses over the depth range of 100-1200m between the last occupation of these stations during the WOCE era (1993) and the 2003 occupation. For example, in the 0-1400m depth range, DIC increases on the order of 2-25 μmol kg^{-1} were observed over the 10 year period between the two cruises. In contrast, the DIC at depths >1500m showed very little change.

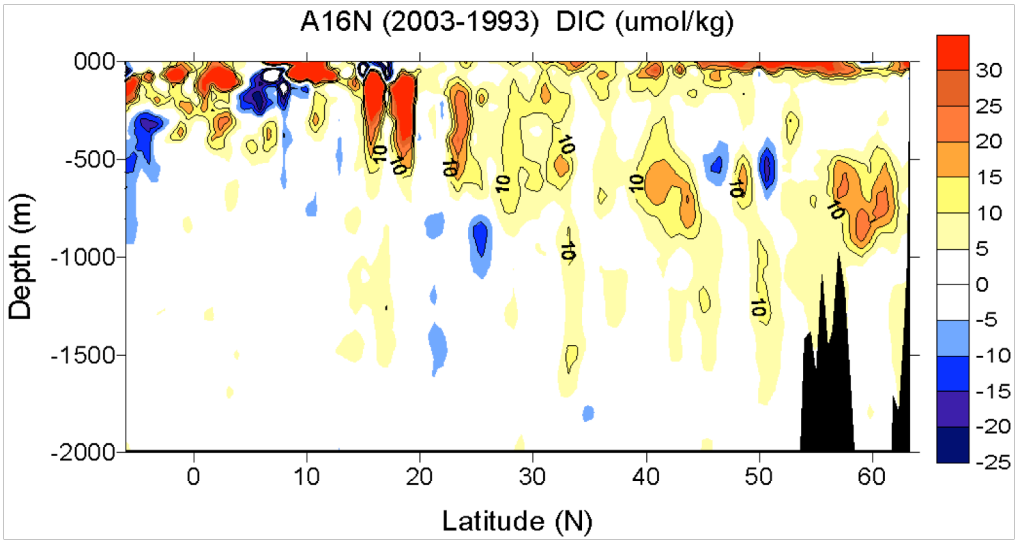

Figure 4. Difference of the dissolved inorganic carbon (DIC in μmol/kg) between 2003 and 1993 as a function of latitude and depth along the A16N cruise track in the North Atlantic.

Similar increases in DIC and AOU were also observed between 100-1200m for the A22/A20 cruises in the western North Atlantic. The increases of DIC in the Subtropical Mode waters (STMW) are greater than expected from invasion of anthropogenic CO_2 from the atmosphere and may be the result of decadal changes in the local circulation in the North Atlantic, and/or changes in new production and remineralization of organic matter along the flow path. As we continue to process the physical and biogeochemical data from these cruises, we should be able to attribute the large-scale changes in the carbon content of the Atlantic Ocean.

2.5.2 Atmosphere-Ocean CO_2 Fluxes

Changes in carbon inventory are the most robust means of assessing sources and sinks but for the oceans these methods are limited to changes over decadal timescales. On average the total dissolved inorganic carbon content (DIC) of the surface ocean increases by about 1.2 μmol kg^{-1}

per year or about 0.05 % over the background. While the accuracy of DIC measurements is about 2 μmol kg^{-1} making detection of the anthropogenic signal in principle possible on shorter time scales, the surface ocean DIC changes by 20 to 50 μmol kg^{-1} seasonally masking changes less than 5 to 10 μmol kg^{-1}.

To assess changes in exchanges between reservoirs on sub-decadal timescale we have to determine the fluxes. The fluxes can be determined from measuring the partial pressure differences of CO_2 between surface ocean and lower atmosphere, Δ pCO_2, and a quantity referred to as the gas transfer velocity that is related to physical forcing and often parameterized with wind speed. Thus, if ΔpCO_2 fields can be determined and used in combination with wind fields, regional fluxes can be obtained.

Creation of flux maps

This approach has been applied successfully using a global climatology of ΔpCO_2 painstakingly developed based on 40-years of ΔpCO_2 data from many investigators (Takahashi et al. 2002). Uptakes based on this climatology range from 1 to 1.9 Pg C yr^{-1} depending on the relationship between gas exchange velocity and wind speed (Table 2). This approach will be used to quantify regional fluxes on seasonal timescale. The implementation will require a significant increase in ΔpCO_2 observations, development of methods to interpolate ΔpCO_2 in time and space, and improvement of algorithms to quantify the gas transfer from wind or other relevant parameters, such as surface roughness, that can be directly observed from remote sensing.

Following a recommendation in the LSCOP plan a surface ocean flux observing system is being put in place with autonomous instrumentation on volunteer observing ships VOS, research ships, and buoys. The LSCOP plan lays out an observing strategy based on scaling analysis that involves sampling of the ocean roughly at 10 degree spacing and monthly intervals. By coordinating efforts with international and national partners this goal will be attainable in the next decade for the North Atlantic, North Pacific and Equatorial Pacific, particularly if we develop methods to increase time and space scales of observation through use of remotely sensed observations. The scheme of implementing such a system utilizing in situ and remotely sensed data is outlined in Figure 5.

Determining and attributing changes in ΔpCO_2

The approach of utilizing remote sensing, algorithms of ΔpCO_2 and gas exchange with remotely sensed products has been utilized in test beds in the Equatorial Pacific and Caribbean Sea (Figures 6 and 7). For the Equatorial Pacific work the algorithms are used in a retrospective fashion to determine the large variations in air-sea flux due to the ENSO cycle.

Limited time series records of surface water pCO_2 levels have shown that for much of the ocean the surface water pCO_2 rises roughly at the same rate as the atmospheric increase implying that the global air-sea flux remains the same. However, changes in the rate of increase are a sensitive indicator of changes in the uptake of the ocean and perturbations in the biogeochemical cycles. Using a historical database of ΔpCO_2 for the Equatorial Pacific Takahashi et al. (2003) determined significantly slower increases in the 80-ties than in the 90-ties that were attributed to a climatic re-organization in the North and Equatorial Pacific referred to as the Pacific Decadal Oscillation (PDO).

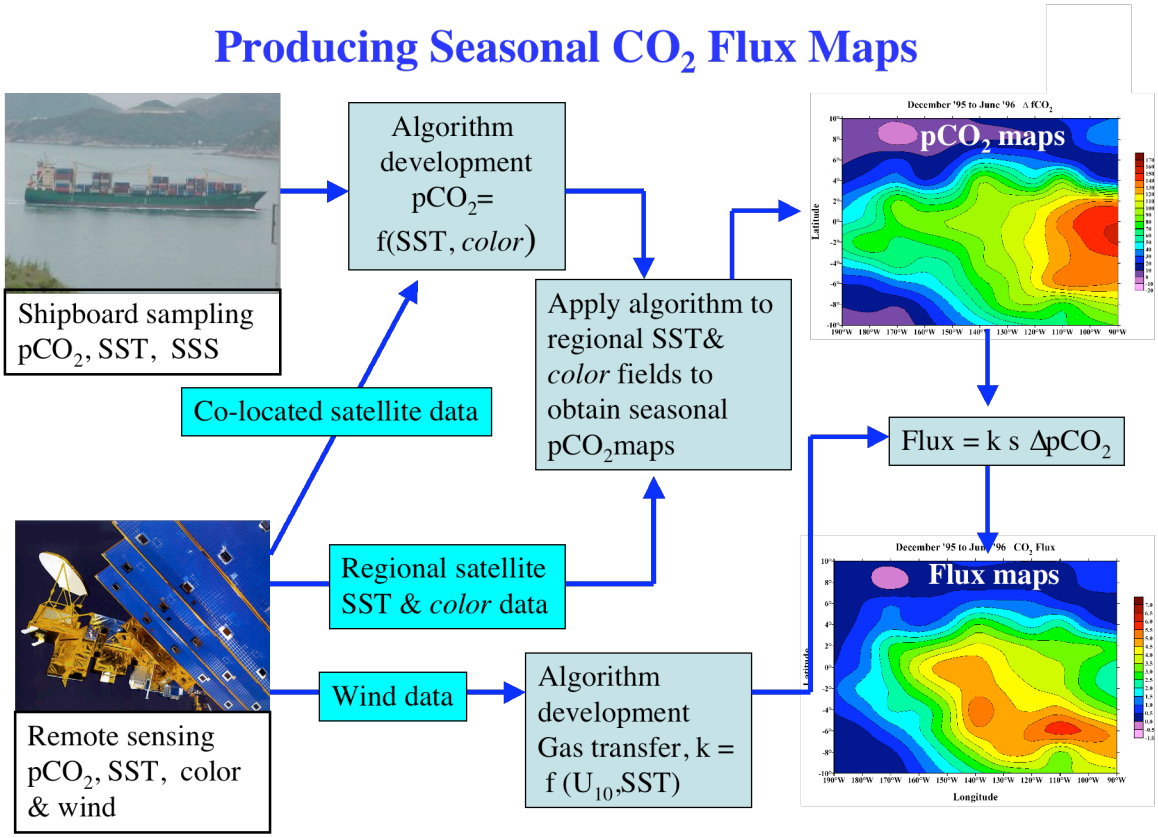

Figure 5. Flow diagram of data and procedures to produce pCO_2 flux maps.

Future plans and milestones

The observational efforts to detect changes in water column inventories and to attribute the causes, and the development of regional CO_2 flux maps are part of well documented and justified integrated carbon plans. The CLIVAR/CO_2 Repeat Hydrography Program has a series of cruises planned for the next decade that will yield sequential basin wide inventory changes for the Atlantic, Pacific, Southern and Indian oceans. The cruise sequence is listed in Table 3. NOAA/COSP has the lead on the cruises for A16S, A16N, P16N, P18 and I8. NOAA participants will perform DIC and pCO_2 measurements on all cruises. Operational Milestones are provided in Table 4.

Table 3. Sequence of CLIVAR/CO_2 Repeat Hydrography cruises in the oceans.

Schedule of US CLIVAR/CO2 Repeat Hydrography Lines (as of 10/04)					
Dates	**Cruise**	**Days**	**Ports**	**Year**	**Contact/Chief Scientist**
					Overall Coordinator: Jim Swift, SIO
6/19/03-7/10/03	A16N, leg 1	22	Reykjavik-Madeira	1	Bullister, NOAA/PMEL
7/15/03-8/11/03	A16N, leg 2	28	Madeira - Natal, Brazil	1	Bullister, NOAA/PMEL
9/15/03-10/13/03	A20	29	WHOI - Port Of Spain	1	Toole, WHOI
10/16/03-11/07/03	A22	21	Port Of Spain - WHOI	1	Joyce, WHOI
6/13/04-7/23/04	P2, leg 1	41	Yokohama-Honolulu	2	Robbins, SIO
7/26/04-8/26/04	P2, leg 2	32	Honolulu - San Diego	2	Swift, SIO
1/11/05-2/24-05	A16S	45	Punta Arenas-Fortaleza	3	Wanninkhof/Doney; NOAA/AOML/WHOI
1/8/05-2/18/05	P16S	40	Tahiti-Wellington	3	Sloyan/Swift, WHOI/SIO
2006	P16N	57	Tahiti-Alaska	4	Feely/Sabine, NOAA/PMEL
austral summer 07	S4P/P16S	25.5	Wellington-Perth	5	
austral summer 07		25.5	Wellington-Perth	5	
2008	P18	32	Punta Arenas-Easter Island	6	
2008		35	Easter Island- San Diego	6	
2008	I6S	42	Cape Town	6	
2009	I7N	47	Port Louis/Muscat	7	future planning
2009	I8S	38	Perth- Perth	7	future planning
2009	I9N	34	Perth- Calcutta	7	future planning
2010	I5	43	Perth - Durban	8	future planning
2010	A13.5	62	Abidjan-Cape Town	8	future planning
2011	A5	30	Tenerife-Miami	9	future planning
2011	A21/S04A	42	Punta Arenas-Cape Town	9	future planning
2012	A10	29	Rio de Janeiro-Cape Town	10	future planning
2012	A20/A22	29	Woods Hole-Port of Spain-Woods Hole	10	future planning

Years 1-6 are funded.

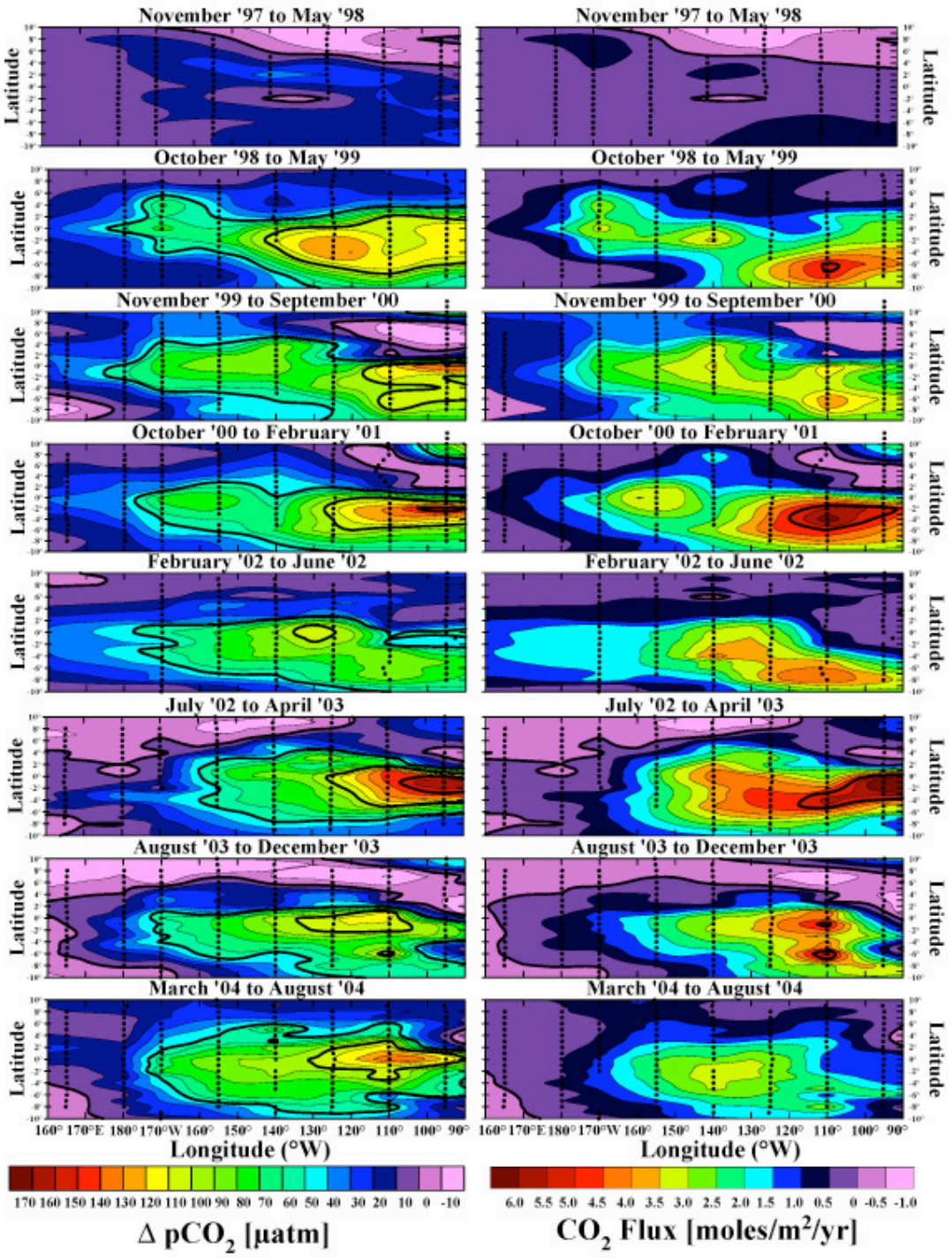

Figure 6. Time Series of ΔpCO_2 (left) and CO_2 fluxes in moles m^{-2} yr^{-1} in the equatorial Pacific from November 1997 thru August 2004. Low CO_2 fluxes are observed during both the strong 1997-98 El Nino and the weak 2002-3 event (Feely et al., in preparation).

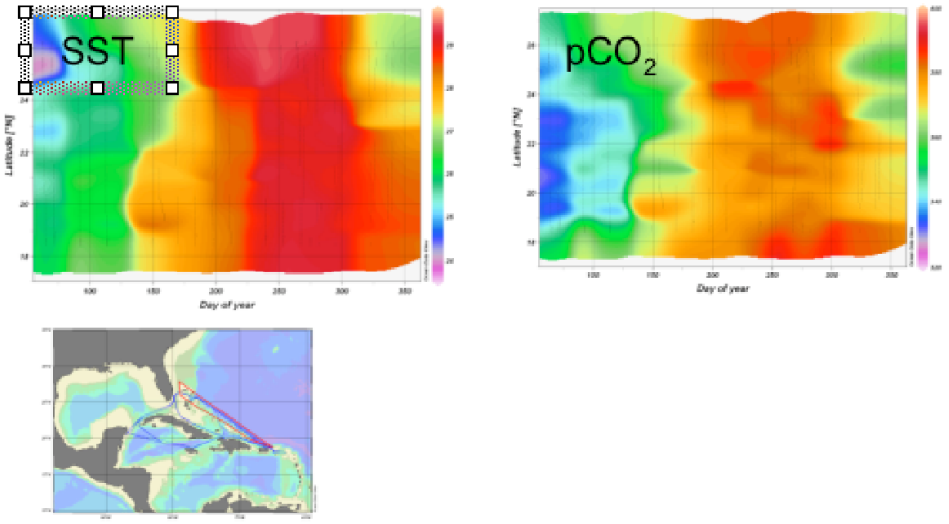

Figure 7. Production of pCO_2 maps in the Caribbean. Empirical algorithms are being developed with parameters that are measured at higher density/frequency (e.g. through remote sensing.). The close correspondence of temperature (left panel) trends and pCO_2 (right panel) along the cruise track (bottom) facilitates robust algorithms to extrapolate the pCO_2 to regional scales (Olsen et al. 2004).

Table 4. Operational milestones of the CLIVAR/CO_2 Repeat Hydrography Program

Summer 2003	Organize and complete the A16N cruise in the North Atlantic and provide leadership (chief scientist), CTD, oxygen, nutrient, total carbon and pCO_2 analysis.
Winter 2003/2004	Provide final CO_2, oxygen, CTD data to the repeat hydrography data center at Scripps.
Summer 2004	Analyze total inorganic carbon on the P2 cruise.
Winter 2004/2005	Provide final total CO_2 data to the repeat hydrography data center at Scripps.
Winter 2004/2005	Organize and complete the A16N cruise in the North Atlantic and provide leadership (chief scientist), CTD, Oxygen, nutrient, total carbon and pCO_2 analysis.
Winter 2004/2005	Analyze total inorganic carbon on the P16S cruise.
Spring 2006	Organize and complete the P16N cruise in the Pacific and provide leadership (chief scientist), CTD, Oxygen, nutrient, total carbon and pCO_2 analysis.

The COSP CO_2 flux map effort focuses on the ΔpCO_2 observations needed to create the seasonal maps. The implementation schedule is presented in Table 5 with the italicized text that will be proposed in FY 05. The effort is starting to incorporate time series on moorings that are critical to determine the higher frequency (< 1-month) temporal variability. Particularly in the coastal oceans and Equatorial Pacific large changes can occur on weekly timescales. The exact balance and number of fixed pCO_2 observing sites vs. ship based (moving) observing platform has not been firmly established. Analysis of the results of the initial surface pCO_2 observing system will be used to optimize spacing, frequency, and mix of observing methods. Optimizing the observing system requires inclusion of measurements of biogeochemical and physical parameters that influence pCO_2 as well in order to investigate extrapolation routines. The added benefit will be that these parameters yield mechanistic information that can be used in prognostic models and interpolation schemes utilizing satellite data. An to end-to end iterative effort starting from observations to interpretation and analysis feeding into improved observing system design and assessing the state of the ocean carbon cycle is critical at this point and attainable within national and international frameworks.

Table 5. Operational milestones pCO_2 project

Fall 2003	Complete installation of pCO_2 system on Skogafoss (Iceland-Norfolk) line AX2
Spring 2004	Complete installation of pCO_2 system and TSG system on Columbus Waikato (Long Beach -New Zealand) line PX13
Summer 2004	Complete installation of pCO_2 system on Oleander (Bermuda-Norfolk)
Winter 2004/2005	Complete standardized data reduction and quality control scheme for all ships Start submitted data to LDEO on routine basis for contextual QC.
Spring 2005	Complete installation of pCO_2 system on Sealand Express (Iceland-Norfolk)
Fall 2005	Complete installation of pCO_2 system on 24N line (Miami-Gibraltar)
Winter 2005/2006	*Install system on VOS ship in North Pacific*
Spring 2006	*Install system on NOAA survey ships in Gulf of Mexico (Gunther) and Bering Sea (Rainer)*

Data for all projects will be distributed to the community at large through a Live Access Server within two years after collecting the data.

National and International linkages

The COSP carbon program is an integral part of national and international programs in carbon cycle research. NOAA's contribution is unique as it is the only program that has the sustained observational effort necessary to constrain sources and sinks and provide input for prognostic models to predict future trends. The international connection for the repeat hydrography effort is through WCRP/CLIVAR and the IGBP/IMBER programs. The former is focused on the physical aspects of climate variability while the latter is geared to the ecological and biogeochemical components. The flux map effort is connected to the SOLAS effort theme 3: Air-Sea Flux of CO_2 and Other Long-Lived Radiatively-Active Gases. International coordination for both aspects of CO_2 COSP will occur through the International Ocean Carbon Co-ordination Project (IOCCP). International ties between the ocean carbon programs and the atmospheric, terrestrial, and human dimension carbon cycle research are provided through the IGBP/WCRP/IHDP Global Carbon Project (GCP).

At a national level the CO_2 COSP effort is part of the US Carbon Cycle Science Plan. Its critical role in the overall US ocean science effort is outlined in the multi-agency implementation plan, the Ocean Carbon and Climate Change plan (Doney 2004). Information about the programs linked to, or a part of, COSP-CO_2 can be found in Table 6.

Table 6. Web sites of the CO_2/COSP program and program partners:

Data sites for pCO_2 data from ships:

AOML	http://www.aoml.noaa.gov/ocd/gcc
PMEL	http://www.pmel.noaa.gov/uwpco2/
LDEO	http://www.ldeo.columbia.edu/res/pi/CO2/

Program sites

CLIVAR:	Climate Variability and Predictability: www.clivar.org
SOLAS:	Surface-Ocean Lower Atmosphere Study: www.uea.ac.uk/env/solas/
IOCCP:	International Ocean Carbon Coordination Project www.ioc.unesco.org/ioccp
IGBP:	International Geosphere-Biosphere Project: www.igbp.kva.se/cgi-bin/php/frameset.php
IMBER:	Integrated Marine Biogeochemistry and Ecosystem Research http://www.igbp.kva.se/cgibin/php/
WCRP:	World Climate Research Program: www.wmo.ch/web/wcrp/wcrp-home.html
GCP:	Global Carbon Project: http://www.globalcarbonproject.org/

References

Bender, M., S. Doney, R.A. Feely, I.Y. Fung, N. Gruber, D.E. Harrison, R. Keeling, J.K. Moore, J. Sarmiento, E. Sarachik, B. Stephens, T. Takahashi, P.P. Tans, and R. Wanninkhof, 2002: A large Scale Carbon Observing plan: In Situ Oceans and Atmosphere (LSCOP), pp. 201, Nat. Tech.Info. Services, Springfield.

Doney, S., 2004: The Ocean Carbon and Climate Change Report, UCAR, Boulder.

Feely, R.A., J. Boutin, C. E. Cosca, Y. Dandonneau, J. Etcheto, H. Y. Inoue, M.Ishii, C. Le Quere, D. Mackey, M. McPhaden, N. Metzl, A. Poisson, and R. Wanninkhof., 2002: Seasonal and interannual variability of CO_2 in the Equatorial Pacific. *Deep Sea Res. II*, **49**, 2443-2469.

Feely, RA., C.L. Sabine, T. Ono, A. Murata, R. Key, C. Winn. M. Lamb, and D. Greeley, 2004: CLIVAR/CO_2 Repeat Hydrography Program: Initial carbon results from the North Pacific Ocean. *Eos Transactions, AGU,* **85**(47)*, Fall Meeting Supplement OS24B-02.*

Houghton, J.T., Y. Ding, D.J. Griggs, M. Noguer, P.J.v.d. Linden, and D. Xiaosu, Climate Change 2001: The Scientific Basis: Contribution of Working Group I to the Third Assessment Report of the Intergovernmental Panel on Climate Change (IPCC), pp. 944, Cambridge University Press, Cambridge, England.

Sabine, C.L., M. Heimann, P. Artaxo, D. Bakker, C.-T.A. Chen, C.B. Field, N. Gruber, C. LeQuéré, R.G. Prinn, J.E. Richey, P.R. Lankao, J. Sathaye, and R. Valentini, 2004a: Chapter 2, Current status and past trends of the global carbon cycle. In SCOPE 62, *The Global Carbon Cycle: Integrating Humans, Climate, and the Natural World*, C.B. Field and M.R. Raupach, Eds., Island Press, Washington D.C., 17–44.

Sabine, C.L., R.A. Feely, N. Gruber, R.M. Key, K. Lee, J.L. Bullister, R. Wanninkhof, C.S. Wong, D.W.R. Wallace, B. Tilbrook, F.J. Millero, T.-H. Peng, A. Kozyr, T. Ono, and A.F. Rios, 2004b: The oceanic sink for anthropogenic CO_2. *Science*, **305**, 367–371.

Sarmiento, J.L., and S.C. Wofsy, 1999: A U. S. carbon cycle plan, pp. 69, UCAR, Boulder.

Takahashi, T., S.G. Sutherland, C. Sweeney, A.P. Poisson, N. Metzl, B. Tilbrook, N.R. Bates, R. Wanninkhof, R.A. Feely, C.L. Sabine, J. Olafsson, and Y. Nojjiri, 2002: Global sea-air CO_2 flux based on climatological surface ocean pCO_2, and seasonal biological and temperature effects, *Deep-Sea Res. II*, **49**, 1601-1622, 2002.

Takahashi, T., S.C. Sutherland, R.A. Feely, and C.E. Cosca., 2003: Decadal variation of surface water pCO_2 in the Western and Central Equatorial Pacific. *Science*, **302**, 852-856.

2.6 SURFACE CURRENT OBSERVATIONS FOR CLIMATE RESEARCH

by Peter Niiler[1] and Nikolai Maximenko[2]

[1]Scripps Institution of Oceanography, La Jolla, California
[2]International Pacific Research Center, Honolulu, Hawaii

Background

A principal scientific objective of the "*Global Drifter Program"* of the NOAA Ocean Climate Observing System is to produce instrumental data records of the near surface velocity of the global oceans (Niiler 2001). The velocity is derived from observing the motion of Argos satellite located drifting buoys that are drogued to 15m depth. Velocity is computed from the six hourly displacements of drifters and these observations are corrected for "slip" of the drogue through water due to forces of wind (and waves) on the surface float and the tether that connects the float to the drogue (Pazan and Niiler 2001). The *Global Drifter Data* Center at the Atlantic Oceanographic and Meteorological Laboratory of NOAA produces and maintains data files from all drifters (8049 up to July 2004) and a *Bibliography* of the research papers which have used these data for understanding ocean circulation physics:
(http://www.aoml.noaa.gov/phod/dac/drifter_bibliography.html).

From 1992 to 2002 enough drifter velocity data was accumulated that a 10-year time-mean circulation could be computed for about 80% of the surface of the globe. These time mean circulation data, together with wind and satellite altimeter observations, were used to compute the absolute sea level map of the world oceans for the 2003 Climate Observation Report (Niiler et al. 2003). This sea level distribution, or surface dynamic topography, has been assimilated in a number of Ocean General Circulation Models (OGCMs) for climate studies. For the 2004 Report we compute and discuss the seasonal mean and El Niño and La Niña anomaly circulation patterns for the tropical Pacific. These circulation data are being used to verify the ocean surface current patterns of the OGCMs, which are employed in the prediction of ENSO.

Tropical Pacific Seasonal Currents

Modern drifter observations in the ocean current systems of the tropical Pacific began in 1978 (Hansen and Paul 1984). Since 1988, an array of over 200 drifters has been maintained within 20 degrees latitude of the equator. The objective was to measure the basin scale seasonal currents so the circulation anomalies during El Niño and La Niña could be determined. On Figure 1a the mean of the 15m depth velocity is computed from the ensemble of 6 hourly observations within 2x5 degree boxes. All the major known current systems of the tropical Pacific are displayed with an accuracy and degree of certainty that has not been possible from any other data source (Niiler et al. 2004).

As an aid to sailing mariners, geographers have named the east-west components of the surface currents on Figure 1a, from south to north, as: the South Equatorial Current, the North Equatorial Countercurrent and the North Equatorial Current. Just as important for climate studies, however, are the north-south components, whose strength and patterns were not known before drifter velocity observations. These poleward flows are driven directly by the Trade Winds (Ralph and Niiler 1999) and they are warmed by solar heating as they move away from the cold, up welled zone on the equator. They then give back their thermal energy to the atmosphere in the center of the Trades. This pattern of heat transfer can be seen by noting on Figure 1a the angle the currents make with the SST distribution that underlies the circulation vectors. If the vector points toward warm water the water parcels absorb heat from the atmosphere, toward cold water if the water parcels give up heat to the atmosphere.

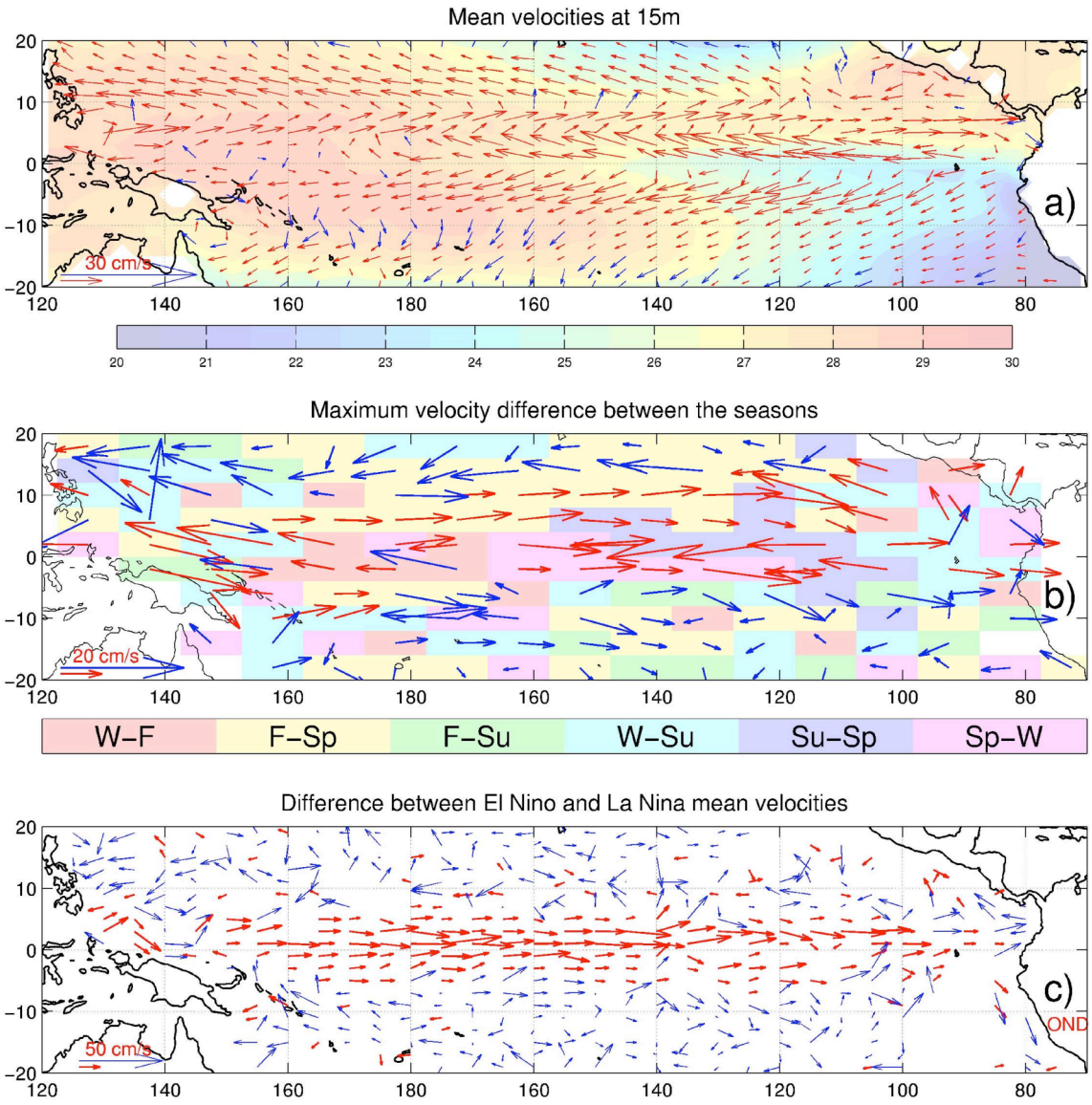

Figure 1. *(a)* Mean current velocities at 15 m depth derived from Lagrangian drifters (vectors) overlaid on mean COADS SST (colors). *(b)* Pairs of boreal seasons (colors), between which the velocity demonstrate the largest differences (vectors). *(c)* Velocity differences between the October-December averages over three El Niño (1991, 1997 and 2002) and three La Niña (1988, 1995 and 1999) events. Vectors that are smaller than 5, 15 and 20 cm/s, correspondingly, are shown on panels *(a)*, *(b)* and *(c)* in blue color.

The summary of the seasonal changes on Figure 1b display that the largest changes are zonally oriented. These occur in the South Equatorial Current between January-March (W) and April-June (Sp) periods and North Equatorial Countercurrent between April-June (Sp) and October-December (F) periods. A more complete description and the dynamical causes for these seasonal changes have not been fully complete, but could be in light of these robust data sets. Changes of zonal currents in the tropics are related most strongly to the wind stress curl changes. A central CLIVAR modeling objective is to understand the seasonal changes of ocean circulation and these data are vital to a verification of this modeling activity.

The El Niño – La Niña Anomalies

The seasons of October-December (F) 1991, 1997 and 2002 characterize the mature El Niño seasons and in 1988, 1995 and 1999 mature La Niña seasons occur during the same months. The largest differences of the ensemble averages of the October-December seasonal velocities for the mature El Niño and mature La Niña years on Figure 1c occur across the entire 5 degree latitude band of the equator. These equatorial La Niña current can be are over 100 cm/sec more to the west than El Niño currents. These changes can be caused directly by reversal or collapse of the Southeast Trade Winds (Ralph et al. 1997) in the western Pacific or equatorial Kelvin waves that are a result of these wind changes. Kelvin waves travel eastward over the entire extent of the equatorial basin so current changes can be remotely forces as well. These anomalous zonal currents are thought to cause anomalous movements of warm water across the equatorial basin (Picaut et al. 2001). Locally these velocity changes were observed with equatorial moorings (Wang and McPhaden 2000), but broad latitude and longitude extent of the changes of equatorial circulation due to the Pacific ENSO were not known before basin scale drifter velocity observations became available.

Future of Circulation Observations

Observations of the movement of drogued drifters will continue within the *Global Drifter Program*. By June 2005 the global array of drifters will be increased to, and maintained for the foreseeable future at, 1250 elements. Together with satellite altimeter and wind observations, these drifter data will continue to provide valuable data sets for the study of the changing circulation patterns of the global near surface circulation.

References

Hansen, D. V., and Paul C. A., 1984: Genesis and effects of long waves in the equatorial Pacific. *J. Geophys. Res.,* **89**, 10431–10440.

Niiler, P., 2001: The World Ocean Surface Circulation. Chapter 4.1 in "*Ocean Circulation and Climate- Observing and Modeling the Global Ocean*", *Ed.* by J. Church, G. Siedler and J. Gould, Academic Press, London. 715pp.

Niiler, P.P., N.A. Maximenko, and J.C. McWilliams, 2003: Dynamically balanced absolute sea level of the global ocean derived from near-surface velocity observations. *Geophys. Res. Lett.,* **30** (22), 2164, doi:10.1029/2003GL018628.

Niiler, P., D.-K. Lee and J.E. Moisan, 2004: "The mechanisms of El Nino SST evolution in the tropical Pacific". *J. Mar. Res*., **62**(6): 741-760.

Picaut, J.M., C. Loulalen, C. Menkes, T. Delcroix, M.J. McPhaden, 1996: "Mechanism of the zonal displacements of the Pacific Warm Pool: Implications for ENSO". *Science,* **274**: 1486-1489.

Pazan, S.E., P.P. Niiler, 2001: "Recovery of near-surface velocity from undrogued drifters". *J. Oc. Atm. Tech.,* **18**(3): 476-489.

Ralph, E.A., K.N. Bi and P.P. Niiler, 1997: "A Lagrangian description of the western equatorial Pacific response to the wind burst of December 1992: heat advection in the warm pool." *J. Climate,* **10**(7): 1706-1721.

Ralph, E.A., P.P. Niiler, 1999: "Wind driven currents in the tropical Pacific". *J. Phys. Oceanogr.,* **29**(9): 2121-2129.

Wang, W. and M.J. McPhaden, 2000: "The surface-layer heat balance in the equatorial Pacific Ocean. Part II: Interannual variability", *J. Phys. Oceanogr.*, **30**(11): 2989-3008.

2.7 AIR-SEA EXCHANGE OF HEAT, FRESH WATER, MOMENTUM

by Robert C. Weller, Woods Hole Oceanographic Institution, Woods Hole, Massachusetts

Abstract

Exchanges of heat, freshwater, and momentum between the ocean and the atmosphere play a key role in determining the climate of the earth and its variability. Our present knowledge of these fluxes is poor, which is evident when high quality time series observations of these air-sea fluxes from a surface mooring are compared against climatological values and against fluxes from models (Fig. 1). The NOAA Climate Observation Program is addressing the need for accurate observations of the exchange of heat, freshwater, and momentum between the ocean and atmosphere by working toward a global array of such high quality surface moorings, known as Ocean Reference Stations. These moorings, together with Volunteer Observing Ships (VOS), will provide the data critical to developing improved maps of the air-sea fluxes; a pilot project has produced improved maps in the Atlantic (Fig. 2). In 2004 progress was made when a third Ocean Reference Station was deployed and work to produce global maps of fluxes began.

The ocean has a distinct role in governing the variability of the earth's atmosphere, land, and ocean. It carries heat poleward from the equatorial regions where the sun shines most strongly. It releases heat and moisture into the lower atmosphere to drive weather patterns, storms and hurricanes, and longer period climate variability that includes the El Niño-Southern Oscillation. The ocean, which covers 70% of the earth, can store 1100 times more heat than the atmosphere due to the larger heat capacity and density of water. The upper 2.5 m of the ocean, when warmed 1°C, thus stores an amount of heat that would raise the entire column of air above it 1°C as well. As a consequence, an anomalously warm region of the ocean has the potential of releasing considerable energy to the atmosphere above and thus driving the weather on short time scales and, if the release of heat persists, altering climate. Energy to drive the atmosphere is also transferred from the ocean by evaporation, and the ocean's role as a source of moisture is critical to understanding weather and climate as well as the global cycle of freshwater. The ocean stores 97% of the earth's water and plays a major role in the global cycle of freshwater that heavily impacts agriculture and human activities; 86% of the evaporation and 78% of the precipitation occur over the ocean. The third exchange between the ocean and atmosphere of interest is that of momentum, the transfer of which determines how the surface winds drive the ocean currents and how the ocean surface provides drag to the atmosphere. The shallow, wind-driven ocean currents are of particular interest because of their role in transporting the surface waters that are warmed and cooled by exchanges with the atmosphere.

One goal of the NOAA Climate Observation Program is to collect long, accurate time series of the air-sea exchanges of heat, freshwater, and momentum at key locations around the world's ocean, aiming toward 16 such sites by 2006 and building to 51 of these sites, known as ocean reference stations. A second goal is to use these accurate observations together with surface meteorological and air-sea flux observations from Volunteer Observing Ships (VOS) to produce daily maps of the air-sea fluxes over the global ocean.

What are the reasons for these goals? First, these maps will show where and how much heat and freshwater are exchanged between the ocean and atmosphere, show how the winds drive the surface currents, and thus quantify the exchanges between the ocean and atmosphere that play important roles in weather, climate, and the global water cycle. With this information we would be able to document the impact on climate of anomalous heat and freshwater loss to the atmosphere by a region of the ocean and to search for the connections across the globe between rainfall and temperature anomalies on land and where and how much heat and freshwater was released from the ocean. At present, due to sparse observations and large uncertainties in the

present estimates of the air-sea exchanges, we cannot (across time scales that range from hurricanes to decadal) determine across the globe whether or not anomalous ocean conditions cause or result from anomalous atmospheric conditions. We look to new, accurate flux maps with good temporal and spatial resolution to show where and when change in the ocean leads or lags change in the atmosphere and leads to climate variability on land; this information is key to improved prediction of climate variability.

Second, the flux maps will provide the surface forcing for numerical ocean models used to investigate oceanic variability and the ocean's role in climate; such models are now forced using climatological surface fluxes or other fields of fluxes that have large uncertainties, which in turn add uncertainty to the results of the ocean modeling. The ocean, as pointed out above, has a large ability to store heat. It also has a three-dimensional circulation that is much slower than that of the atmosphere, with the deep waters being exposed to the atmosphere only every 100 years or so. Accurate surface forcing is needed as we look to improve the ability of these ocean models to properly simulate the mixing, overturning, and decadal and longer term transport, storage, and release back to the atmosphere of heat and freshwater.

Third, atmospheric models are now forced at the sea surface with sea surface temperature fields and use their own parameterizations to develop surface fluxes of heat, fresh water, and momentum. By comparison with data from the ocean reference stations that are being deployed by the NOAA Climate Observation Program, the air-sea fluxes in these atmospheric models are found often to have large differences from the actual fluxes. This needs to be addressed because many ocean modelers use the atmospheric model flux fields as their surface forcing and also because the role of the ocean in weather and climate variability in these atmospheric models and in climate models that use the same or similar code may not be well represented. Moreover, accurate fields of the surface exchanges are required for evaluation of the ability of coupled ocean-atmosphere climate models, such as those used in IPCC (Intergovernmental Panel on Climate Change) predictions of future climate change, to simulate present day climate. Such evaluations are necessary if we are to have confidence in the future climate change scenarios predicted by these models.

Fourth, surface flux fields are widely used in observational studies by the oceanographic research community studying large scale ocean circulation and its impact on climate, in synthesis with sub-surface measurements, to determine the transports of water and heat across basin scale ocean sections. In particular, the fields of momentum flux are required to determine the wind-driven or Ekman component of the ocean transport, and the fields of heat, fresh water, and momentum flux are needed to provide surface forcing conditions for analyses of hydrographic (ocean temperature and salinity) data which use inverse techniques to estimate the transports of water with different, characteristic temperatures and salinities.

Finally, the accurate time series from the ocean reference stations serve several key functions: 1) provide accurate long time series of known accuracy at key locations which are of high value as records of variability and change in the coupling of the ocean and atmosphere, 2) help to calibrate and validate remote sensing, 3) provide the ability to examine the realism of the air-sea fluxes in numerical weather and climate models, 4) provide accurate records of the surface forcing to be used in studies of oceanic response to and interaction with the atmosphere, and 5) provide critical points across the ocean basins to use as standards and anchor sites to develop the global air-sea flux fields through the synthesis of data from the diverse sources needed to achieve daily, global fields.

The context for this element of the Climate Observation Program can be illustrated by Figure 1, which compares time series of air-sea fluxes from a surface mooring of the type being deployed at the Ocean Reference Stations. Monthly means of wind stress (momentum flux) and net heat flux from two state of the art numerical weather models, one from the National Center for Environmental Prediction (NCEP) and one from the European Centre for Medium Range Weather Forecasts (ECMWF) are plotted against the monthly means from the buoy and monthly means from flux fields developed at Southampton Oceanography Centre (SOC) from VOS observations. Note not only how large the differences in net heat flux are between the NCEP and ECMWF monthly means and those of the buoy but also that the NCEP heat fluxes have the wrong sign during June and July. Indeed the ECMWF model indicates through the year about 50 W m^{-2} less heat into the ocean than observed, and the NCEP has a negative bias of about 100 W m^{-2}. Errors of this size have been seen at other sites. Yet, recent ongoing efforts to understand the dynamics of the upper ocean and the ocean's role in climate, such as the World Ocean

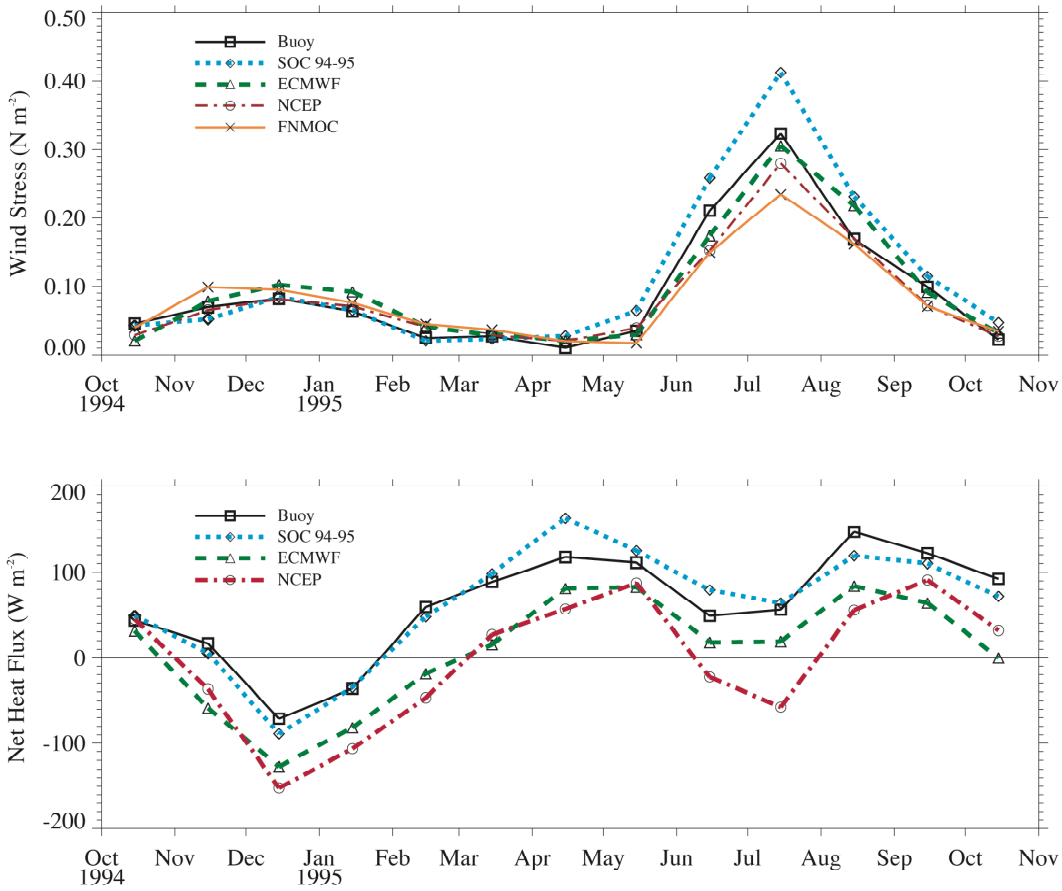

Figure 1. Monthly mean wind stress (momentum exchange) (upper) and net heat flux (positive into the ocean) at a mooring deployed in the northern Arabian Sea for one year.

Circulation Experiment (WOCE), the Tropical Ocean-Global Atmosphere Program (TOGA), and the Climate Variability (CLIVAR) Program have identified the need for monthly mean net heat flux estimates to be available with accuracy of better than 10 W m^{-2}. Consistent accuracy targets for precipitation and wind stress are 0.01 mm hr^{-1} and .01 N m^{-2}, respectively. These lead to target accuracies for sea and air temperature of 0.1°C, for wind speed of better than 5%, for

relative humidity of better than 3%, for incoming shortwave of better than 10 W m^{-2}, and for incoming longwave of better than 5 W m^{-2}. Some of the errors cancel, and these target accuracies typically allow the 10 W m^{-2} goal in the net heat flux to be met at present. A more challenging objective for the future of this effort motivated by the desire to better understand long term climate change would be to resolve mean values of the net heat flux well enough to be able to sense shifts in the surface radiation budget associated with changes in greenhouse gases and aerosols, thus requiring the reduction of errors in the net heat flux to approximately 4 W m^{-2}.

This element of the Climate Observation Program is in its initial phase. The goals are to deploy and maintain the Ocean Reference Stations and, using these time series as the critical accurate reference observations, to produce global maps of the air-sea fluxes of heat, freshwater, and momentum. The challenge is a significant one, requiring cruises to deploy and maintain each Ocean Reference Station once per year, requiring dedicated on the land and at sea calibration efforts to obtain the sought after accuracies in these unattended surface moorings, and also requiring well-instrumented VOS that cross the ocean basins to obtain essential complementary information about the spatial variability in the surface meteorological and air-sea fluxes and in the differences between these observed fields and the model and remotely-sensed fields used to synthesize global maps.

At present, one Ocean Reference Station is operating under the stratus clouds off the coast of northern Chile (20°S, 85°W), one in the tropical western North Atlantic (15°N, 51°W), and one north of Hawaii (23°N, 158°W). Near term plans are to complement the sensors on four existing TAO-TRITON sites in the equatorial Pacific to qualify them as Ocean Reference Stations. A pilot project has been conducted, using past buoy, model, and satellite data, to test and develop the methodology of producing air-sea fluxes fields on basin scales. Figure 2 shows a comparison of the long-term (1988 to 1997) mean sum of the latent and sensible heat flux components from a new flux product developed by L. Yu at Woods Hole Oceanographic Institution (WHOI) with the SOC climatology and mean fields from ECMWF and NCEP. The WHOI product produced by data assimilation methodology compared the best against the buoy data available from this period. This pilot project affirmed the approach being taken, and Yu is now developing global flux fields.

As yet, the observations made under this component are sparse. The data are withheld and not used in preparation of model fields by the operational weather and climate modeling centers. This is done so that the Ocean Reference Station time series can serve as an independent assessment of model performance and thus to stimulate the ongoing dialog that will motivate improvements to these models. The sparse Ocean Reference Stations are building evidence of biases and errors in the models at the few sites now occupied. A milestone for the project will be when the deployed buoys cover many of the critical weather and climate regimes of the global ocean and thus can be used to identify and fix problems in these models common to all sites as well as to identify issues unique to specific regimes.

With sufficient funding and with new observatory technology to be developed under the Ocean Observatory Initiative of the National Science Foundation, the deployment of the planned numbers of Ocean Reference Stations is entirely feasible. Each site will require a regular, once per year commitment of ship time and of on land and at sea calibration. Significant milestones will be achieved when the Ocean Reference Stations in each basin provide time series from the meteorological and air-sea regimes characteristic of those basins. When that is accomplished, the time series from these moorings will provide compelling evidence to drive the process of partnering with the atmospheric modeling community to improve the realism of those models and to produce basin scale flux fields of the desired accuracy.

Linkage to the climate and weather modeling communities is being actively pursued, as are ties to research programs seeking long time series. In part this is done through dialog with the NSF Observatory Initiative. It is also done through the Partnership for Ocean Global Observations (POGO), through participation in planning for the Global Earth Observing System, and through participation in the World Climate Research Program Working Group on Surface Fluxes (WGSF). The WGSF especially supports the ties between the Ocean Reference Stations and the international climate and weather modeling efforts and the development of improved accuracies in surface meteorological and air-sea flux measurements. The addition of attitude (pitch, roll, heave, and mean tilts) measurements and of turbulent flux capabilities to the Ocean Reference Stations are identified as next steps to be taken that would determine the comparability of the radiation observations from the buoys with the land based observations of the Surface Radiation Network and would improve flux accuracies in the low and high wind speeds where the bulk formulae methods have remaining uncertainties.

These time series sites should be accompanied by accurate measurements from the ships that deploy and recover the mooring to provide in-the-field calibration of the moored time series. They should also be accompanied by improved measurements from selected VOS to obtain direct observations of the spatial variability of the surface meteorological and air-sea flux fields. Practical considerations require the implementation of a hierarchy of VOS observations systems. The state of the art instrumentation of two to three long cross-basin ship lines (with preference for the high resolution XBTs lines) in each ocean basin will provide estimates of high absolute accuracy. A few hundred ships recruited under the VOSClim program will have improved instrumentation and sufficient documentation to allow any measurement biases to be quantified and corrected through comparison with the Ocean Reference Stations. The majority of the international VOS fleet (some six thousand ships) will continue to provide basic observations over large areas of the world oceans which must be verified against the higher quality observations from the specially chosen ships and buoys. These observing efforts should be accompanied by quality control efforts, by close interaction with the atmospheric modeling centers and those working up remotely-sensed fields at the ocean surface, and by production of global fields of the air-sea exchanges of heat, freshwater, and momentum that are made available to the research and operational communities.

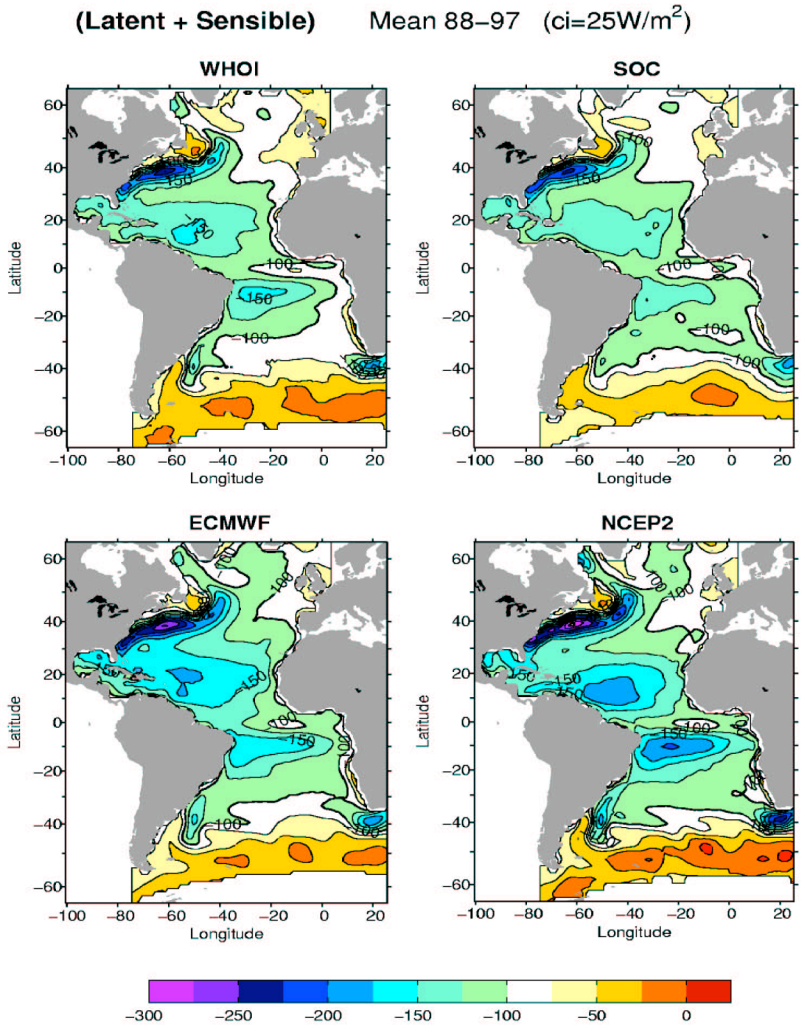

Figure 2. Four maps of the long-term (1988-1997) sum of latent and sensible heat flux components in the Atlantic basin. WHOI was produced by L. Yu at WHOI and validated against buoy data. SOC is a climatological product based on VOS data; ECMWF and NCEP2 are analyses based on those numerical weather prediction models.

Acknowledgement

This section on air-sea exchange of heat, fresh water and momentum was written with input from Drs. Peter Taylor and Simon Josey of the Southampton Oceanography Centre, UK, Dr. Chris Fairall of the NOAA Environmental Technology Laboratory, Boulder, Colorado, and Dr. Frank Bradley of the Commonwealth Scientific and Industrial Research Organization (CSIRO), Canberra, Australia.

2.8 SEA ICE EXTENT AND THICKNESS

by Ignatius Rigor[1] and Jackie Richter-Menge[2]

[1]University of Washington, Seattle, WA
[2] Cold Regions and Research Engineering Laboratory, Durham, New Hampshire

Abstract
Although the extent of sea ice is limited to the higher latitudes of the Arctic (Fig. 3) and Antarctic, and covers only 7% of the global oceans, sea ice has a profound affect on the climate of the mid-latitudes in which we live. Sea ice affects many aspects of the global climate system through its role in maintaining global temperatures at levels which make life on earth sustainable and by its effect on the global thermohaline circulation which transports heat around the earth.

The extent and thickness of sea ice on the global ocean has been decreasing dramatically during the last few decades, and the last three summers have exhibited record low sea ice extent on the Arctic Ocean. The summer of 2002 set the record minimum for the Northern Hemisphere, while the summer of 2004 (Fig. 6) was very close to this record. The precipitous decline of sea ice has been attributed to the long-term effects of changes in wind, which have blown most of the older, thicker sea ice out of the Arctic Ocean, and warmer temperatures melting sea ice. These changes have been associated with the increases in greenhouse gases in the atmosphere.

Introduction
Understanding the state of sea ice on the global ocean is important since changes in sea ice may foreshadow changes in global climate and affect the global climate system.

The Arctic has been argued to be a harbinger of global climate change since global climate models predict that when the concentrations of CO_2 in the atmosphere doubles the Arctic would warm by more than 5°C, compared to a warming of 2°C for subpolar regions (Manabe et al. 1991), thus the increases in global temperature can be detected in the Arctic sooner than in lower latitudes. This enhanced warming of the Arctic was attributed to the ice-albedo feedback, a process in which an anomalous decrease in sea ice would increase the exposed area of the darker ocean, increasing the amount of sun light absorbed, thus warming the ocean, melting more sea ice, and amplifying the initial perturbations.

Although the extent of sea ice is limited to the higher latitudes of the Arctic and Antarctic, and covers only 7% of the global oceans, sea ice has a profound affect on the climate of the mid-latitudes in which we live. Sea ice affects many aspects of the global climate system through its role in maintaining global temperatures at levels, which make life on earth sustainable and by its effect on the global thermohaline circulation which transports heat around the earth (Aagaard and Carmack 1994).

Figure 1 shows some of the connections between the Arctic and the global climate system. Excess heat from the sun absorbed at lower latitudes is transported poleward by the atmosphere and ocean where it is radiated back out to space. Sea ice has a higher albedo (reflectivity) than the darker ocean (Fig. 2), and hence its presence reduces the amount of sunlight absorbed by the sea ice covered ocean, thus allowing the earth cool more efficiently. However, sea ice also insulates

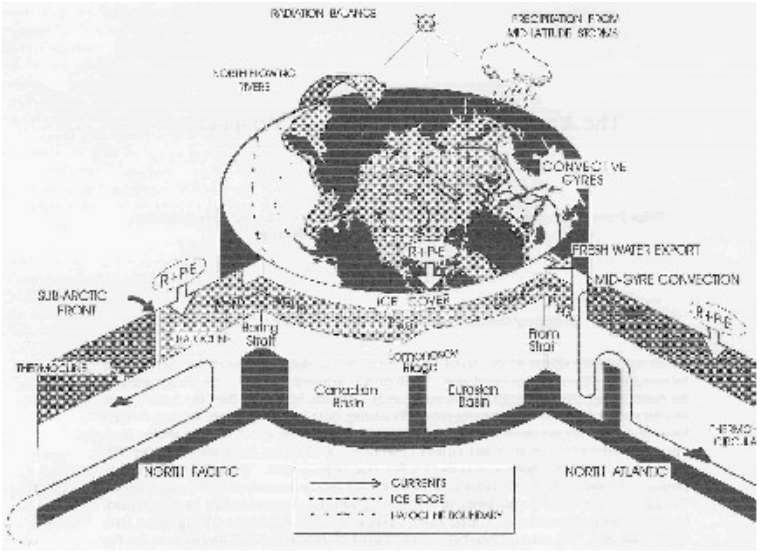

Figure 1. Schematic of Arctic connections to global climate. In the horizontal place, the extent of sea ice in winter is shown by the shaded region and the mean surface circulation by arrows. Sections of the North Pacific and the North Atlantic extend through Bering and Fram straits, respectively. The subarctic front separates the salt-stratified upper waters of the arctic and the subarctic oceans from the temperature-stratified upper waters of the subtropical oceans. The components of the freshwater balance include runoff (R), precipitation (P), evaporation (E), storage in the upper North Pacific (F_{NP}), and Arctic Ocean (F_{AO}), and the North Atlantic (F_{NA}), and the horizontal freshwater fluxes (Q_{in} and Q_{out}). Shaded ovals indicate the present sites of convection in the Greenland and Iceland seas (from Aagaard and Carmack 1994).

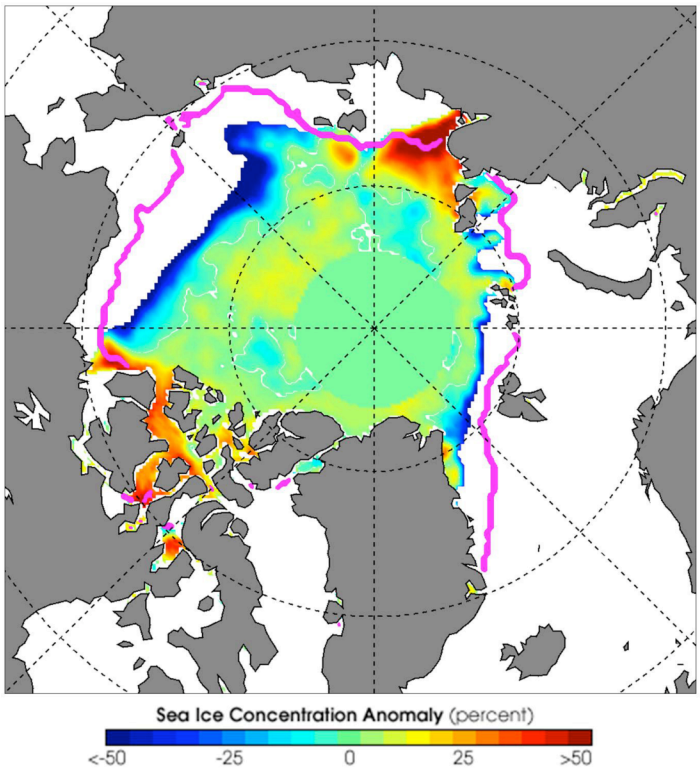

Figure 2. The record minimum sea ice extent in the Northern Hemisphere in September 2002. Image provided by National Aeronautic and Space Administration, http://www.nasa.gov.

the colder atmosphere from the warmer ocean thus reducing the amount of heat lost to space. These opposing processes underscore the complexity of the Arctic and global climate system.

Sea ice affects the global thermohaline circulation through its effect on the salt and fresh water budget of the global ocean (Aagaard and Carmack 1994). As sea ice grows, salt is expelled from the sea ice into the ocean. Since sea ice primarily grows on the Arctic Ocean, it expels most of its salt in this area. The fresher sea ice is then transported towards Fram Strait and the convective regions in the Greenland and Labrador seas (North Atlantic, Figs. 1–3). The melting ice provides a source of fresh water, which is less dense than sea water and may hinder the formation of deep water, thereby slowing the global thermohaline circulation, thus reducing the amount of heat transported by the ocean from the tropics to the higher latitudes (Aagaard and Carmack 1994; Kwok and Rothrock 1999; Belkin 2004).

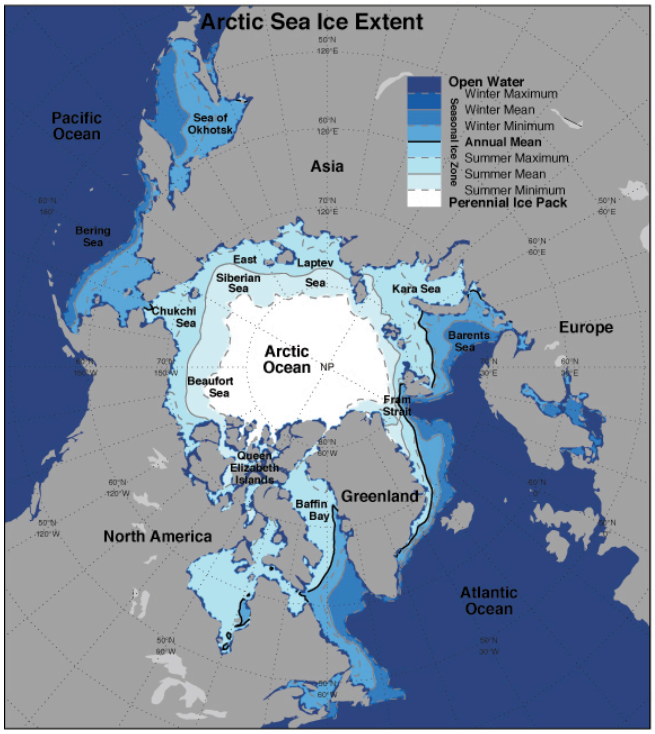

Figure 3. Climatological mean sea ice extent and geography of the Arctic. The extent of sea ice varies by season and from year to year. The seasonal mean sea ice extent lines define the boundary within which sea ice has been observed during at least half the seasons on record (1901 – 2002), the seasonal minimum lines define the boundary within which sea ice has been observed during all seasons, and seasonal maximum lines define the boundary within which sea ice has been observed at least once (Rigor 2004).

Sea ice also has a direct and significant impact on wildlife and people. Many species and cultures depend on the sea ice for habitat and subsistence. The lack of sea ice in an area along the coast may expose the coast line to ocean waves which may threaten low lying coastal towns and accelerate the rate of erosion (Lynch et al. 2003). And from a global economic viewpoint, the lack of sea ice during summer makes the Arctic more accessible for navigation; these shipping routes are as much as 60% shorter from Europe to Asia and the west coast of America, compared to the tradition routes through the Suez and Panama canals (ACIA 2004).

Climatology of Sea Ice

The state of sea ice in the global climate system can be summarized by its areal extent and thickness, which vary with the seasons and from year-to-year. For the Arctic, the extent of sea ice can readily be estimated from the observational records from 1901 to 1999, compiled by Walsh (1978, updated) and from passive microwave satellite data, which are available from 1979 to the present (Comiso 1995, updated). The average extent of sea ice estimated from these data varies from 7.5 x 10^6 km^2 during the summer minimum in September (Fig. 3), when sea ice in the Arctic is typically only found in the interior of the Arctic Ocean and in the Greenland Sea, to 15.5 x 10^6 km^2 during the winter maximum in March when ice in the Arctic extends south to cover the Sea of Okhotsk, the northern reaches of the Bering Sea, Baffin Bay, the Labrador Sea and a part of the North Atlantic.

For the Antarctic, long-term records of sea ice extent are limited to the satellite data. Sea ice extent ranges from 3.8 x 10^6 km^2 during the Southern Hemisphere summer minimum in March to 19 x 10^6 km^2 during the winter maximum in September (Comiso 2003). In contrast to the Arctic, most of the sea ice in the Antarctic grows during winter and does not persist from year-to-year.

In comparison to observations of sea ice extent, long-term records of sea ice thickness are limited in space and time to data collected by occasional submarine cruises under the sea ice and field studies on the sea ice, by ice profiling sonars which are moored to the sea floor, and by buoys drifting with the sea ice. However, using satellite altimeter data, which are available from 1993–2001, Laxon et al. (2003) were able to estimate the climatology of Arctic sea ice thickness. They show that the sea ice typically ranges from 1–5 m in thickness, depending on the region, season and year. The ice is thickest along the Canadian Archipelago where sea ice tends to raft against the coast, and thinnest north of Siberia and Alaska where the ice tends to drift away from the coast.

In the Antarctic, Wadhams (1994) reported that sea ice in the Antarctic is typically less 0.6 m, and large ridges of sea ice are rare. The thinnest sea ice is typically found on the periphery of the sea ice pack, which are at warmer latitudes, while the thickest sea adjacent to the continent where the sea ice is sporadically compressed against the coast (Hass 2003). Since Antarctic sea ice is much thinner than in the Arctic, this limits the reliability of satellite altimeters for estimating sea ice thickness over the Southern Ocean.

Variations in Sea Ice

The state of the Arctic sea ice pack is determined by the effects of the atmosphere and ocean upon the sea ice on various time scales. As the sea ice drifts over the Arctic Ocean, its motion is driven primarily by the surface winds, which account for 70% of the day-to-day variance (Thorndike and Colony 1982). On time scales of days to weeks, wind stresses from storms (Shy and Walsh 1996) produce ridges, which thicken sea ice, and areas of open water, which quickly freeze up during winter. Together, these changes act to increase the overall volume of sea ice within a specified area. Ridging tends to occur preferentially during storms, when the wind stress is strong enough to produce large deformations in the sea ice. The number of storms that any given parcel of ice has experienced is cumulative, and hence the amount of ridged ice tends to increase with the age of the ice. The thicker, ridged ice provides stronger insulation for the atmosphere, but a significant amount of heat is still lost to the atmosphere through the cracks in which new sea ice may grow. During spring and summer, the presence of open water allows more solar energy to be absorbed and stored in the ocean mixed layer, thereby prolonging the melt season, and further increasing the annually integrated absorption of solar radiation.

Many of the changes in Arctic climate and sea ice on all time scales have been attributed to the Arctic Oscillation (AO, Thompson and Wallace 1998), which has been identified as the primary

mode of variability of Northern Hemisphere atmospheric circulation. Over the Arctic Ocean, the AO explains more than 54% of the variance in sea level pressure during winter, and 36% during winter and thus many of the changes in Arctic climate such as the increases in surface air temperature and the decreases in sea ice extent and thickness are highly correlated with variations in the AO through the advection of heat and redistribution of sea ice by the wind (Rigor et al. 2002).

Dramatic changes in Arctic sea ice have been documented during the last few decades. Sea ice thickness has decreased by over 40% when the submarine ice profiling sonar records from the 1993–1997 are compared to the records from 1958–1976 (Rothrock et al. 1999). The annual average extent of sea ice has decreased by 8% per decade, and these decreases are larger during summer, 15–20% per decade over the past 30 years (ACIA 2004). Taken together, these studies imply a precipitous decline in total volume of sea ice on the Arctic Ocean. The decline of Arctic sea ice has been attributed to the warmer air temperatures that have been observed (e.g., Rigor et al. 2000, and Jones et al. 1999), which may have thinned and decreased the area of sea ice (ACIA 2004), but there is also some evidence that changes in the circulation of sea ice on the Arctic Ocean driven by changes in winds over the Northern Hemisphere are also important in explaining the recent minima in summer sea ice extent. In contrast, the trends in Antarctic sea ice extent from 1979 to 2000 are insignificant (Comiso 2003).

The last three summers have exhibited record low sea ice extent on the Arctic Ocean. The summer of 2002 set the record minimum for the Northern Hemisphere, while the summer of 2004 was close to the record and had less sea ice over the Arctic Ocean than in 2002, but more sea ice was observed in the Canadian Archipelago and in the Laptev Sea. In Figure 4 we show the trends in summer Arctic sea ice concentration from 1979–2002 (Rigor and Wallace 2004). The strongest trends are observed north of Alaska, and are typically associated with winds coming from southeast, which carry warm continental air onto the Arctic Ocean, and also blow the sea ice away from the coast towards the northwest (e.g., Drobot and Maslanik 2003). However, during the summer of 2002, the air was actually colder over this area, and the winds came from the northwest, which tended to blow the sea ice towards the Alaskan coast and yet a record minimum in sea ice extent was observed.

To explain this apparent discrepancy between the atmospheric forcing and sea ice extent during the summer of 2002, Rigor and Wallace (2004) hypothesized that there may have been a change in the character of the sea ice drifting towards the Alaskan coast. Given the paucity of observations of sea ice thickness, they used the drift of buoys to estimate the age of sea ice as a proxy for sea ice thickness (sea ice thickens with age). In this study, they showed that the area covered by older, thicker sea ice decreased dramatically in the early 1990's with the step to high Arctic Oscillation conditions. The winds during this period blew most of the older, thicker sea ice out of the Arctic Ocean, and new, thinner sea ice grew in its place. Then during the recent years, this younger, thinner sea ice was observed to drift towards the Alaska coast, where the extensive decrease in sea ice extent was observed during the summer of 2002 and 2003, even though temperatures were locally colder than normal. Rigor and Wallace (2004) argue that the sea ice recirculating towards the Alaskan coast is simply not thick enough to survive the summer. The

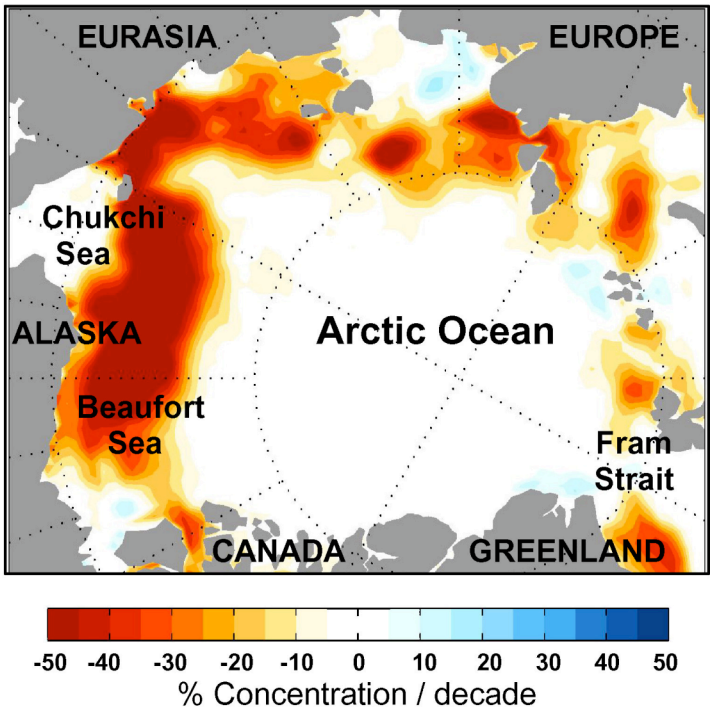

Figure 4. Trends in September sea ice concentration from 1979–2002. Adapted from Rigor and Wallace (2004).

age and thickness of sea ice explains more than half of the variance of summer sea ice extent. The younger, thinner state of most of the sea ice on the Arctic Ocean persists through today.

Rigor and Wallace (2004) show that the recent minima in Arctic sea ice extent may be attributed more to a change in atmospheric circulation sweeping most of the older, thicker sea ice out of the Arctic Ocean, rather than warmer temperatures melting sea ice. However, this does not imply that the decline of Arctic sea ice is not related to the increase in greenhouse gases, since the changes in atmospheric circulation have been attributed to the AO, and there is a growing amount of evidence that greenhouse warming favors high AO conditions.

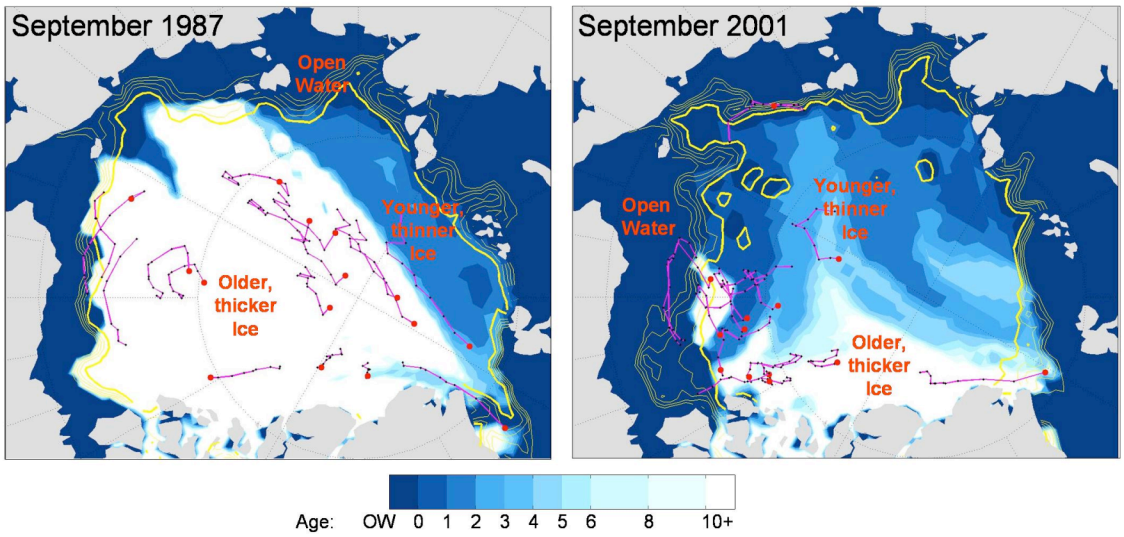

Figure 5. Estimated age of sea ice on the Arctic Ocean in 1987 & 2001. Adapted from Rigor and Wallace (2004).

References

Aagaard, K. and E. C. Carmack, 1994: The Arctic Ocean and climate: A perspective. The Polar Oceans and Their Role in Shaping the Global Environment: The Nansen Centennial Volume, O.M. Johannessen, R. D. Muench, and J. E. Overland, Eds., Amer. Geophys. Union, pp. 5 – 20.

ACIA, 2004: *Impacts of a Warming Arctic: Arctic Climate Impacts Assessment*. Cambridge University Press, 139 pp.

Belkin, I. M., 2004: Propagation of the "Great Salinity Anomaly" of the 1990s around the northern North Atlantic. *Geophys. Res. Lett.*, **31**.

Comiso, J.C., 1995: SSM/I ice concentrations using the Bootstrap algorithm. NASA Report 1380.

Comiso, J., 2003: Large-scale Characteristics and Variability of the Global Sea Ice Cover. Sea Ice, An Introduction to its Physics, Chemistry, Biology, and Geology, D. N. Thomas & G. S. Dieckmann Eds., Blackwell.

Drobot S.D., and J.A. Maslanik, 2003: Interannual variability in summer Beaufort Sea ice conditions: Relationship to winter and summer surface and atmospheric variability. *J. Geophys. Res.,* **108(C7),** 3233, doi: 10.1029/2002JC001537.

Haas, C., 2003: Dynamics versus Thermodynamics: The Sea Ice Thickness Distribution. Sea Ice, An Introduction to its Physics, Chemistry, Biology, and Geology, D. N. Thomas & G. S. Dieckmann Eds., Blackwell.

Jones, P.D., M. New, D.E. Parker, S. Martin, and I.G. Rigor, 1999: Surface air temperature and its changes over the past 150 years. *Rev. Geophys.* **37(C2)**, 173-200.

Kwok, R., and D. A. Rothrock, 1999: Variability of Fram Strait ice flux and North Atlantic oscillation. *J. Geophys, Res.,* **104(C3)**, 5177 – 5189.

Laxon, S., N. Peacock & D. Smith, 2003: High interannual variability of sea ice thickness in the Arctic region. *Nature*, **425**, 947 – 950.

Lynch, A.H., E.N. Cassano, J.J. Cassano, L.R. Lestak, 2003: Case studies of high wind events in Barrow, Alaska: climatological context and development processes. *Mon. Wea. Rev.*, **131**, 719-732.

Manabe, S., R. J. Stouffer, M. J. Spellman, and K. Bryan, 1991: Transient response of a coupled ocean-atmosphere model to gradual changes of atmospheric CO_2, I. Annual mean response. *J. Climate,* **4**, 785-818.

Rigor, I.G., R.L. Colony, and S. Martin, 2000: Variations in Surface Air Temperature in the Arctic from 1979-1997. *J. Climate*, **13**, no. 5, pp. 896 - 914.

Rigor, I.G. and J.M. Wallace, 2004: Variations in the Age of Sea Ice and Summer Sea Ice Extent. *Geophys. Res. Lett.,* **31**, doi:10.1029/2004GL019492.

Rigor, I.G., J.M. Wallace, R.L. Colony. 2002: Response of sea ice to the Arctic Oscillation. *J. Climate,* **15***, 18*, 2648 – 2663.

Rigor, I.G., Interdecadal Variations in Arctic Sea Ice, *Ph. D. Dissertation,* Univ. of Washington, Seattle, pp. 100, 2004.

Rothrock, D.A., Y. Yu, and G.A. Maykut, 1999: Thinning of Arctic sea ice. *Geophys. Res. Lett., 26*, 3469–3472.

Shy T.L., and J.M. Walsh, 1996: North Pole ice thickness and association with ice motion history. *Geophys. Res. Lett.* **23**, 2975–2978.

Thompson, D. W. J., and J. M. Wallace, 1998: The Arctic Oscillation signature in the wintertime geopotential height and temperature fields. *Geophys. Res. Lett.*, **25(9)**, 1297–1300.

Thorndike, A. S., and R. Colony, 1982: Sea ice motion in response to geostrophic winds. *J. Geophys. Res.*, **87(C8)**, 5845–5852.

Wadhams, P., 1994: Sea ice thickness changes and their relation to climate. The Polar Oceans and Their Role in Shaping the Global Environment: The Nansen Centennial Volume, O.M. Johannessen, R. D. Muench, and J. E. Overland, Eds., Amer. Geophys. Union, pp. 337–362.

Walsh, J.E., 1978: A data set on Northern Hemisphere sea ice extent. World Data Center-A for Glaciology (Snow and Ice), "Glaciological Data, Report GD-2", part 1, pp. 49–51.